Redox Control over Acyl Hydrazone Photoswitches

Supporting information

Ivica Cvrtila, Hugo Fanlo-Virgós, Gaël Schaeffer, Guillermo Monreal Santiago, and Sijbren Otto

Centre for Systems Chemistry, Stratingh Institute, University of Groningen, Nijenborgh 4, 9747 AG Groningen, The Netherlands

E-mail: s.otto@rug.nl

Phone: +31 (0)50 363 4233. Fax: +31 (0)50 363 4296

Table of contents

1. Starting materials

All starting materials, unless stated otherwise, were purchased from Sigma Aldrich or TCI, and used without purification. UPLC grade eluents and TFA for UPLC and UPLC-MS analysis were bought from Biosolve.

2-Formylpyridine (**B**) was purified by distillation (b.p. 179 °C; collected at 179 – 191 °C) to remove products of oxidation by atmospheric oxygen.

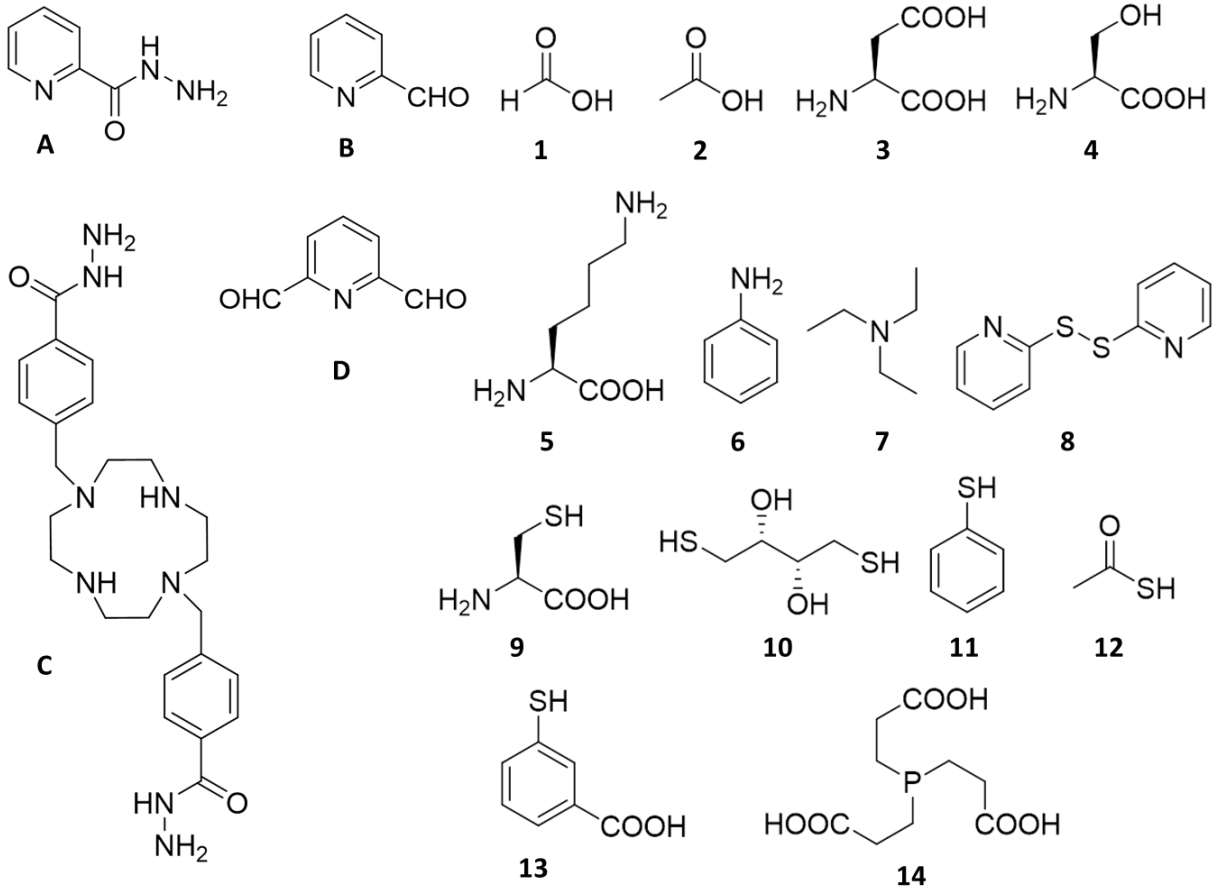

Scheme S1. Materials used for the experiments in this research: picolinic hydrazide (**A**), 2-formylpyridine (**B**), cyclen dihydrazide (**C**), 2,6-diformylpyridine (**D**), formic acid (**1**), acetic acid (**2**), aspartic acid (**3**), serine (**4**), lysine (**5**), aniline (**6**), triethylamine (**7**), 2,2'-dipyridyldisulfide (**8**), cysteine (**9**), dithiothreitol (**10**), thiophenol (**11**), thioacetic acid (**12**), 3-mercaptobenzoic acid (**13**), and TCEP (**14**).

1.1 Synthesis of 4,4'-((1,4,7,10-tetraazacyclododecane-1,7-diyl)bis(methylene))di(benzohydrazide) (C)

Glyoxal protected 1,4,7,10-tetraazacyclododecane (190 mg, 1.00 mmol) and methyl-4-(bromomethyl)benzoate (687 mg, 3.00 mmol) were stirred in dry 1.0 mL CH_3CN overnight. After filtering and evaporating the solvent, the crude product was recrystallized from water (500 mg, 77% yield). Hydrazine monohydrate (2.5 mL) was added and the mixture was refluxed for 2 hours. Hot

water was added (25 mL) to dissolve the product and the final solution was left at 4 °C to allow the product precipitate (355 mg, 99% yield). M.p. 199.3–201.8 °C. ^{1}H-NMR (400 MHz, DMSO): δ 9.78 (s, 2H), 7.85 (d, *J* = 8.4 Hz, 4H), 7.44 (d, *J* = 8.4 Hz, 4H), 7.19 (br s, 2H), 4.51 (br s, 4H), 3.79 (s, 4H), 2.59 (s, 16H). ^{13}C-NMR (100 MHz, DMSO): δ 166.0 (2xO=C(NH-)-), 142.9 (2xC_{quat}), 132.5 (2xC_{quat}), 129.2 (4xCH), 127.4 (4xCH), 60.9 (2xCH_2), 51.7 (4xCH_2), 47.0 (4xCH_2). HR-MS calcd (M+H^+) 469.3034, HR-MS found (M+H^+) 469.3029.

2. Analytical Methods

2.1. NMR

NMR spectra were obtained on a Varian AS 400 MHz instrument. ^{1}H chemical shifts are reported as δ in ppm relative to residual protonated solvent resonances. ^{13}C chemical shifts are reported as δ in ppm and measured relative to solvent references. Coupling constants are reported in Hertz.

2.2. UPLC/UPLC-MS

UPLC analyses were performed on Waters Acquity UPLC H-class and I-class systems equipped with a PDA detector. For the analyses a reverse phase UPLC columns (Acquity BEH Shield RP18, 1,7 µm, 2.1 × 150 mm;) were used, with UPLC grade water (A) and acetonitrile (B) as eluents (both modified with 0.1 % TFA). UV absorbance was monitored at 240, 242, or at 300 nm, and the column temperature was kept at 45 °C. Injection volume was 1.0 µL, flow 0.400 mL/min with the samples being drawn directly from the hydrazone solutions. The elution method is shown in Table S1.

Time (min	% (A)	% (B)
0	90	10
1	84	16
7.5	73	27
8.5	5	95
9	5	95
10	90	10
12	90	10

Table S1. Elution method for UPLC(-MS) analysis of the hydrazone solutions.

UPLC-MS analyses were performed on a Waters Acquity UPLC H-class system (UPLC setup as described previously) coupled to a Waters Xevo-G2 TOF. The mass spectrometer was operated in positive ES mode, with capillary, sampling cone, and extraction cone voltages kept at 2.5 kV, 30 V, and 4 V, respectively. Source and desolvation temperatures were set to 150 °C and 500 °C, respectively. Nitrogen was used both as cone (5 L/min) and desolvation gas (800 L/min).

2.3. UV/Vis measurements

UV/Vis spectra were recorded on a Jasco V-650 spectrometer, using quartz cuvette with the optical path of 1 cm.

3. Preparation and characterization of the hydrazones

3.1. Preparation of buffers

Ammonium acetate buffer solution was prepared by dissolving ammonium acetate in doubly distilled water, adjusting the pH to 4.0 by acetic acid, and by adding more water for the final concentration of ammonia to equal 100 mM.

Ammonium formate buffer was prepared in the same way as ammonium acetate buffer, using ammonium formate and formic acid.

3.2. Preparation of hydrazone solutions

Linear hydrazone (**AB**) solutions were prepared by mixing equal volumes of 2.0 mM solutions of **A** and **B** in ammonium acetate buffer (20 mM, pH = 4.0). Mixed solutions were left to equilibrate for at least an hour prior to UV irradiation and isomerization experiments.

Linear hydrazone (**AB**) for initial UV irradiation experiments was prepared from **A** and **B** following a literature procedure[S1] (47.54 mg (19 %) yield, loss probably due to extensive washing). A 1.0 mM solution of the hydrazone was prepared by dissolving the solid in doubly distilled water.

Macrocyclic hydrazone libraries ((**CD**)$_n$) were prepared by dissolving cyclen dihydrazide **C** (3.0 mM) and 2,6-diformylpyridine **D** (3.0 mM) in ammonium acetate buffer (50 mM) or in ammonium formate buffer (50 mM) and then mixing the solutions in 1:1 ratio. Alternatively, instead of the buffer, doubly distilled water was used, and the cyclen solution was acidified with 1 M HCl to set the pH to 4.0. The library concentrations mentioned in the main text and the SI are always expressed as concentrations of the tetramers, as they are the dominant species in the libraries.

Solid mixture of (**CD**)$_n$ oligomers for initial UV irradiation experiments was prepared by dissolving 11.1 mg (0.0176 mmol) **A** and 2.38 mg **B** (0.0176 mmol) in 4.00 mL water and acidifiying the solution with 10 µL 1M HCl. The solution was left standing for two weeks and the fine precipitate that formed was collected over a sintered glass funnel. Yield: 5.67 mg (58.2 %).

3.3. Preparation of I_2/KI solutions

I_2/KI solutions were prepared by dissolving I_2 in an aqueous solution of KI, with the final concentration of I_2 10 mM, and of KI 20 mM. The concentration of the solution mentioned in the main text and SI always refers to I_2, as KI functions only as solubilizer, by formation of triiodide anions.

3.4. Characterization of the hydrazones

UPLC analysis both of *in situ* prepared **AB**, and of aqueous solutions of **AB** previously isolated as solid, showed only two peaks (Fig 1a in the main text), and the UV spectra thereof were consistent with those previously reported (Figure S1, see also Figure S24a).[S1]

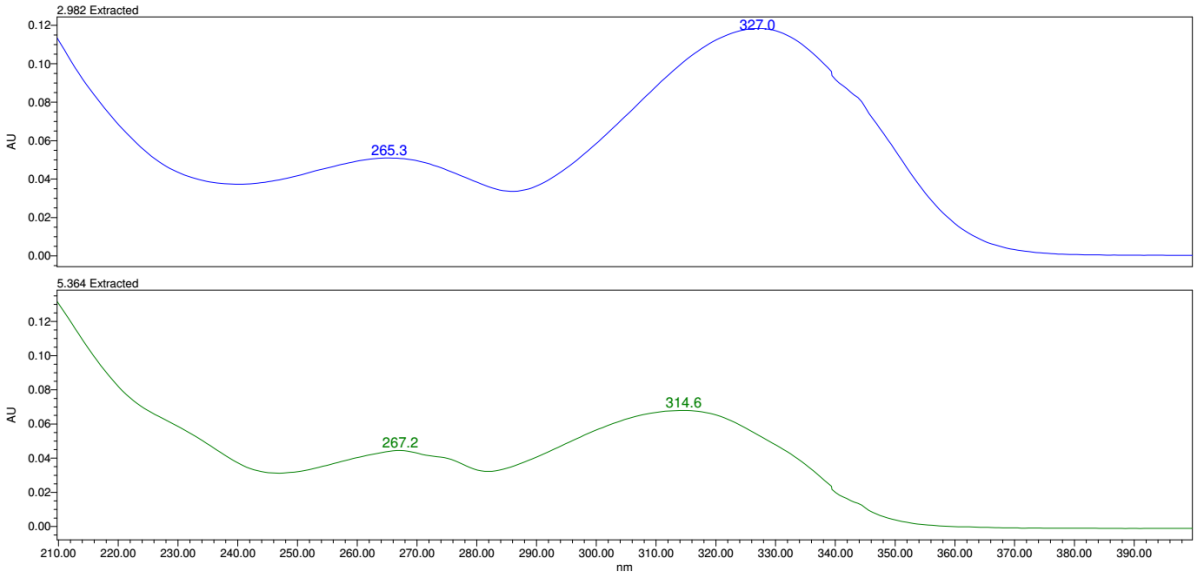

Figure S1. UV spectra of the UPLC peaks corresponding to *E*-**AB** (above) and *Z*-**AB** (below).

Macrocyclic oligomers formed from **C** and **D** were identified by UPLC-MS analysis of two libraries. The first library (**CD-L1**) used for the analysis was made by mixing 3.0 mM solutions of **C** and **D** in ratio 1.05 : 0.95, acidifying the mixture with 1M HCl to set the pH to 4.0, and then diluting the solution with water in ratio 1:4. The final solution was analyzed after standing on the bench for 2 weeks. Analysis revealed the presence of at least four tetramers, seven hexamers, and fifteen octamers (see Figures S2 and S3, details on MS spectra in Figures S4-S16).

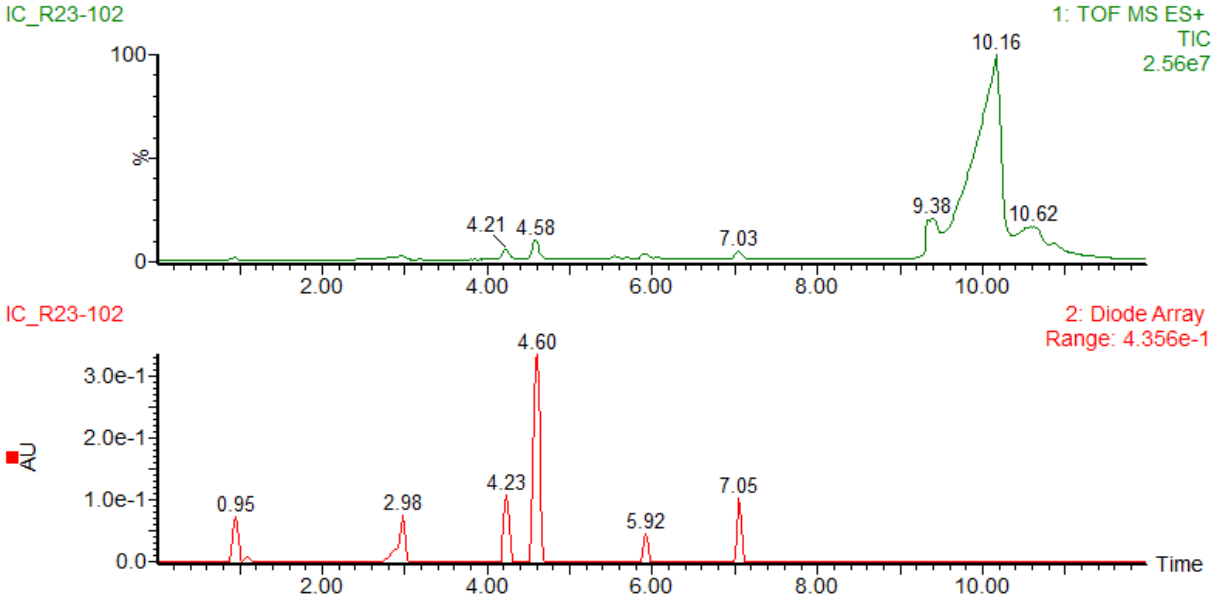

Figure S2. Chromatogram of the (**CD**)$_n$ library **CD-L1**. Total ion count (above) and UV signal (240 nm) (below).

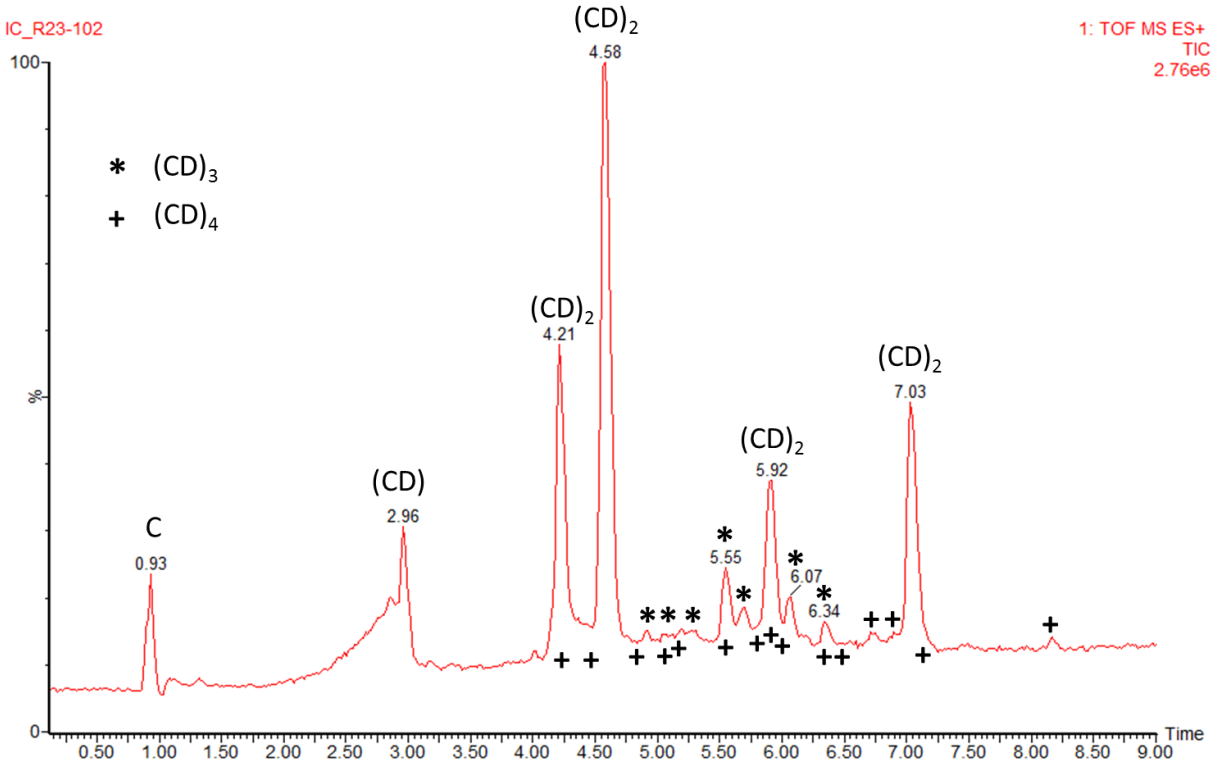

Figure S3. Chromatogram of the (**CD**)$_n$ library **CD-L1**. Expanded region of the TIC signal with assignment of all identified library members (four tetramers, seven hexamers, and fifteen octamers).

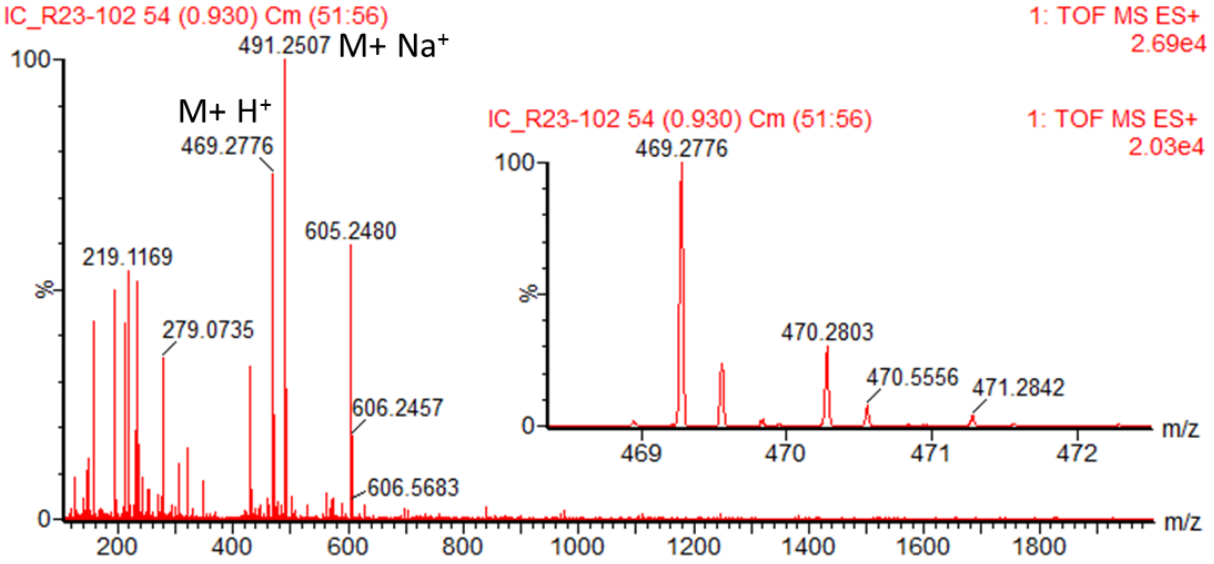

Figure S4. UPLC-MS analysis of library **CD-L1**. Mass spectrum of the peak at 0.93 min, belonging to **C** (*m/Z* ($M+H^+$): calc. 469.3034; obs. 469.2776); inset shows the *m/Z* peaks of the monoprotonated **C**.

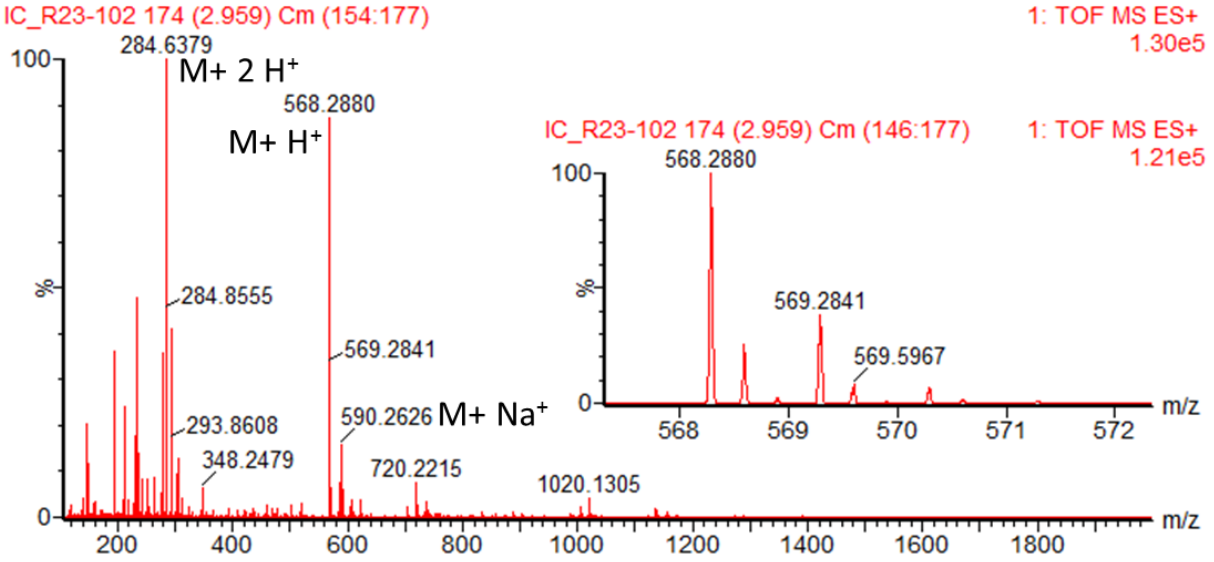

Figure S5. UPLC-MS analysis of library **CD-L1**. Mass spectrum of the peak at 2.96 min (2.0 – 3.0 min), belonging to (**CD**) (*m/Z* ($M+H^+$): calc. 568.3143; obs. 568.2880); inset shows the *m/Z* peaks of the monoprotonated (**CD**).

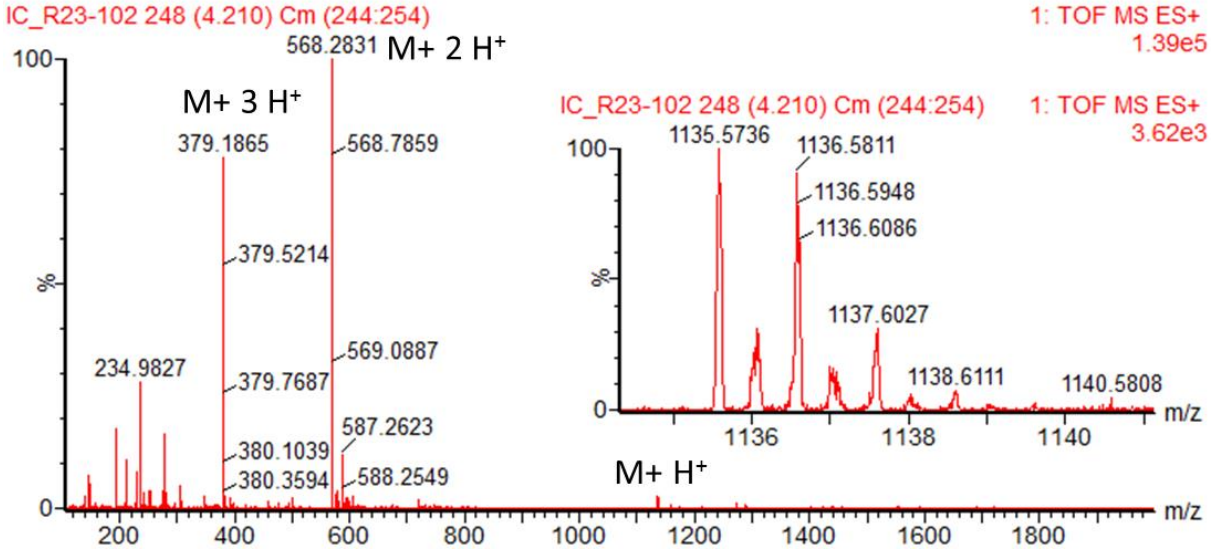

Figure S6. UPLC-MS analysis of library **CD-L1**. a) Mass spectrum of the peak at 4.21 min, belonging to $(\mathbf{CD})_2$ (*m/Z* ($M+H^+$): calc. 1135.6214; obs. 1135.5736); inset shows the *m/Z* peaks of the monoprotonated $(\mathbf{CD})_2$.

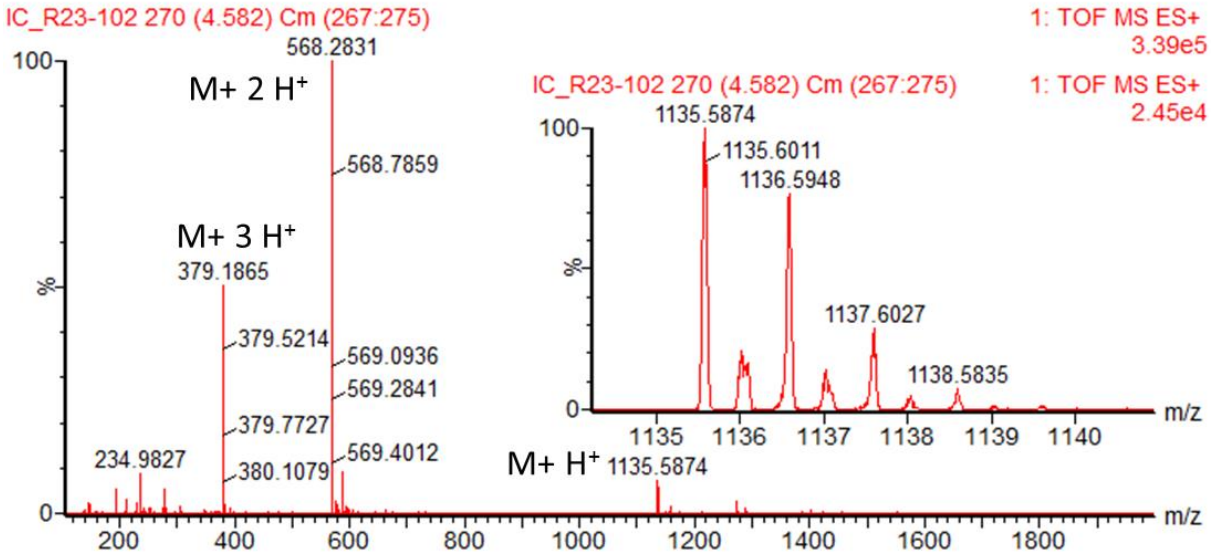

Figure S7. UPLC-MS analysis of library **CD-L1**. Mass spectrum of the peak at 4.58 min, belonging to $(\mathbf{CD})_2$ (*m/Z* ($M+H^+$): calc. 1135.6214; obs. 1135.5874); inset shows the *m/Z* peaks of the monoprotonated $(\mathbf{CD})_2$.

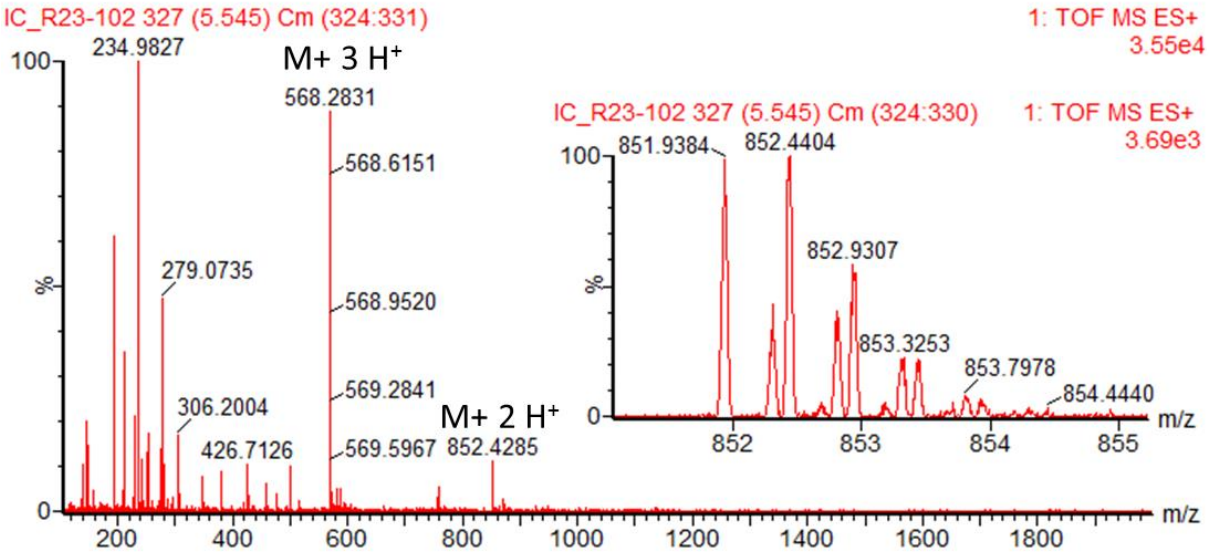

Figure S8. UPLC-MS analysis of library **CD-L1**. Mass spectrum of the peak at 5.55 min, belonging to $(\mathbf{CD})_3$ (*m/Z* ($M+2H^+$): calc. 851.9678; obs. 851.9384); inset shows the *m/Z* peaks of the diprotonated $(\mathbf{CD})_3$.

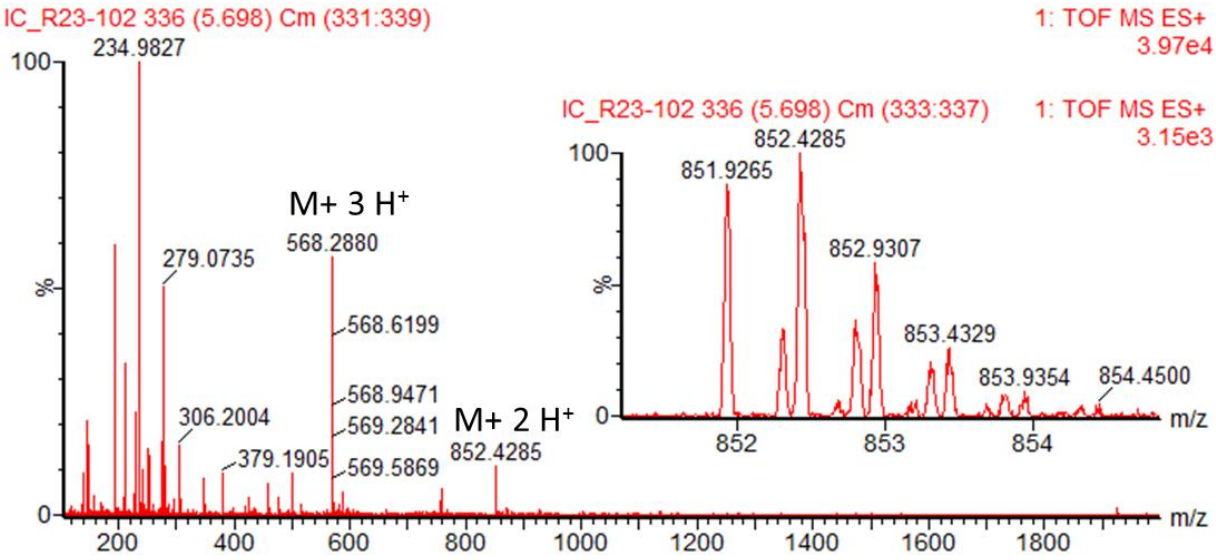

Figure S9. UPLC-MS analysis of library **CD-L1**. Mass spectrum of the peak at 5.70 min, belonging to $(\mathbf{CD})_3$ (*m/Z* ($M+2H^+$): calc. 851.9678; obs. 851.9265); inset shows the *m/Z* peaks of the diprotonated $(\mathbf{CD})_3$.

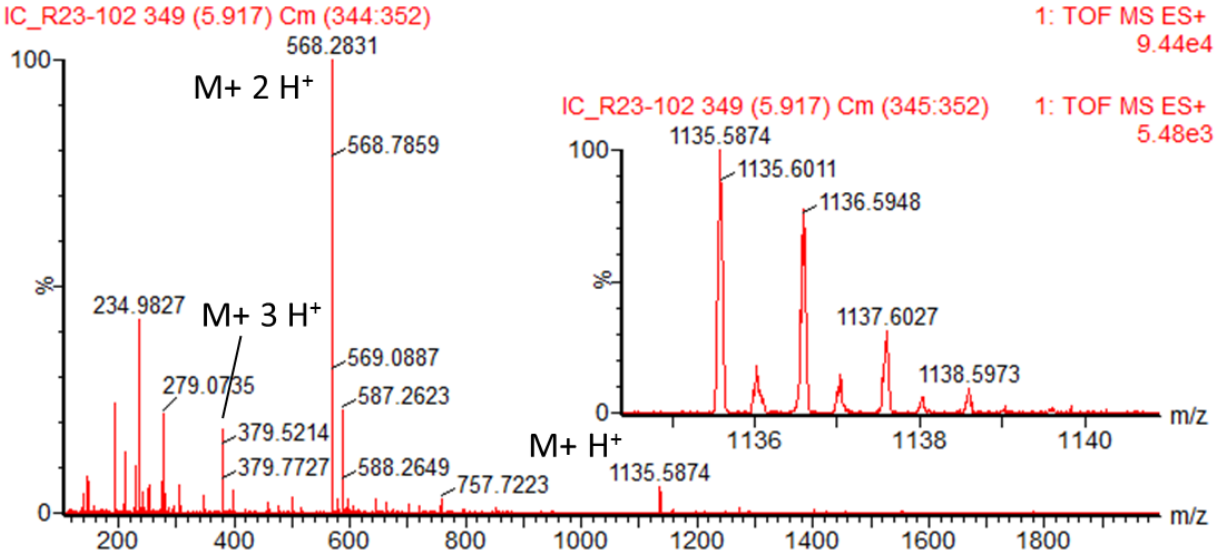

Figure S10. UPLC-MS analysis of library **CD-L1**. Mass spectrum of the peak at 5.92 min, belonging to $(\mathbf{CD})_2$ (*m/Z* ($M+H^+$): calc. 1135.6214; obs. 1135.5874); inset shows the *m/Z* peaks of the monoprotonated $(\mathbf{CD})_2$.

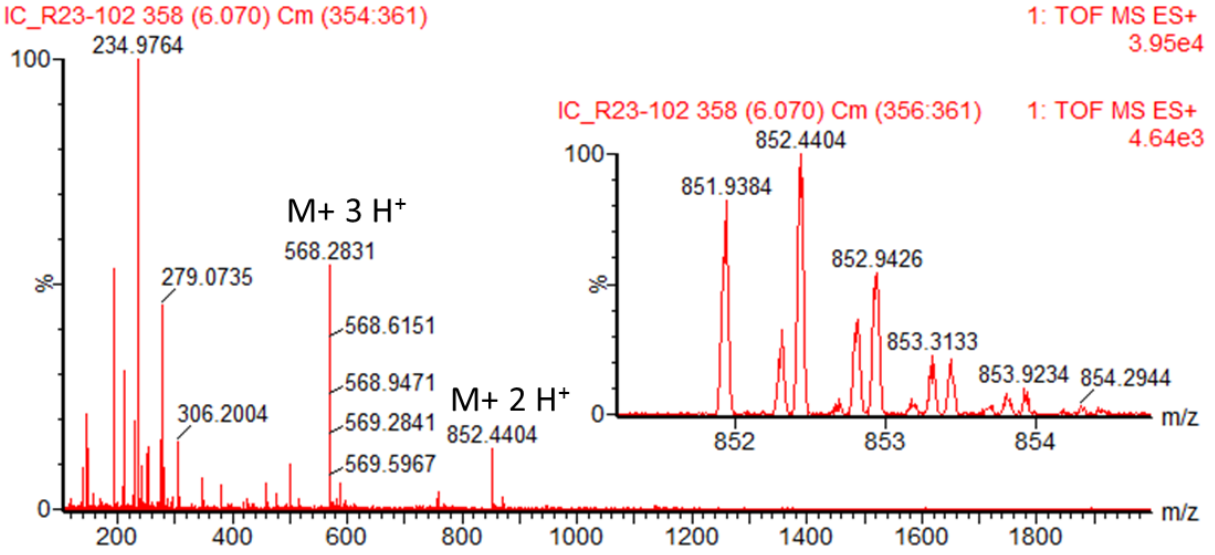

Figure S11. UPLC-MS analysis of library **CD-L1**. Mass spectrum of the peak at 6.07 min, belonging to $(\mathbf{CD})_3$ (*m/Z* ($M+2H^+$): calc. 851.9678; obs. 851.9384); inset shows the *m/Z* peaks of the diprotonated $(\mathbf{CD})_3$.

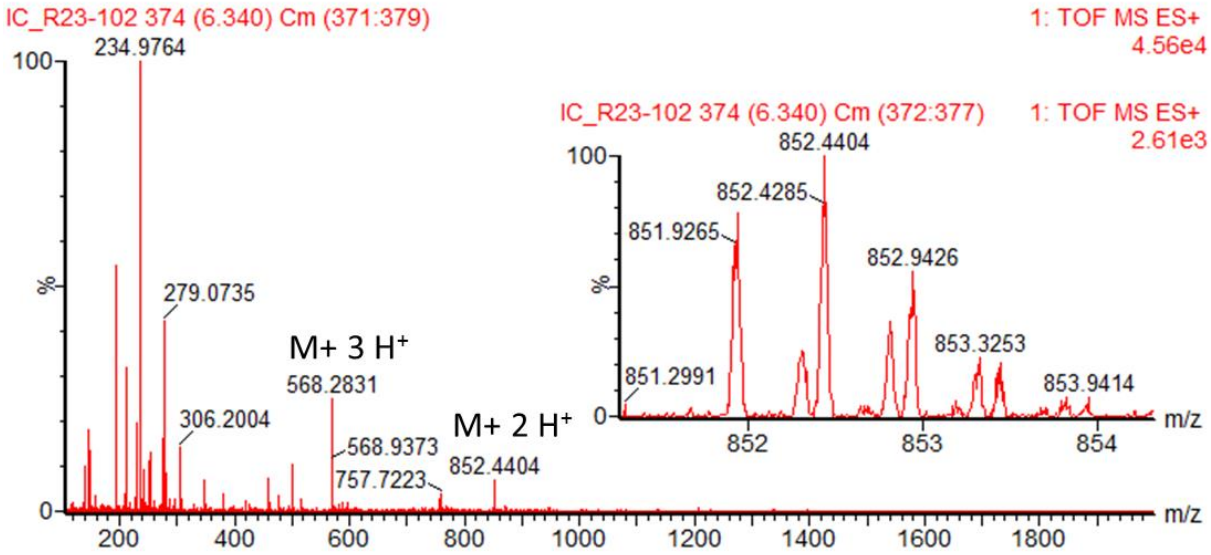

Figure S12. UPLC-MS analysis of library **CD-L1**. Mass spectrum of the peak at 6.34 min, belonging to $(\mathbf{CD})_3$ (*m/Z* ($M+2H^+$): calc. 851.9678; obs. 851.9265); inset shows the *m/Z* peaks of the diprotonated $(\mathbf{CD})_3$.

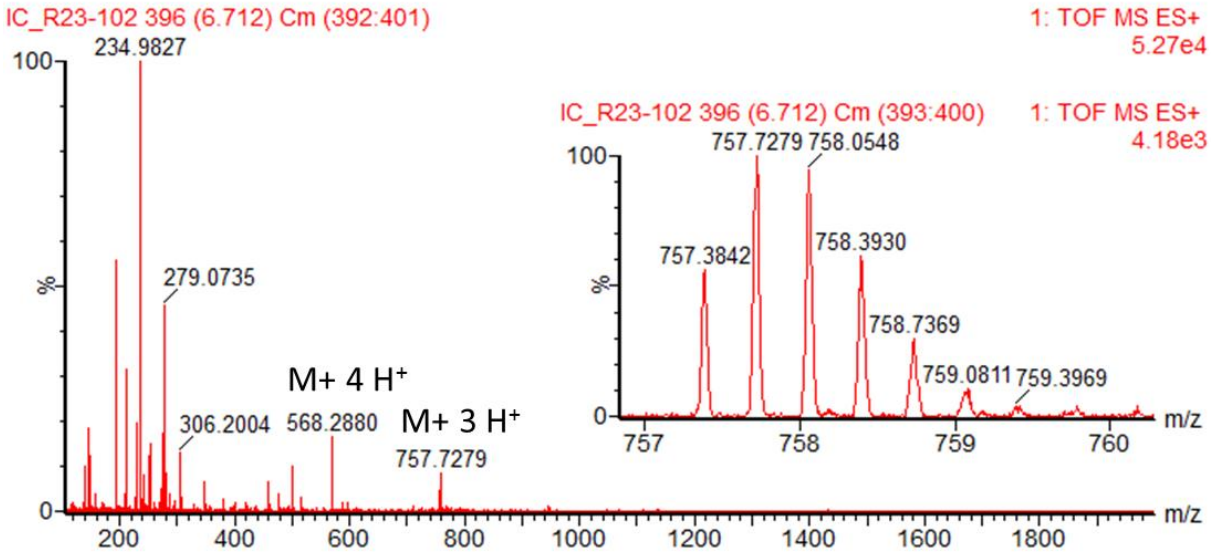

Figure S13. UPLC-MS analysis of library **CD-L1**. Mass spectrum of the peak at 6.71 min, belonging to $(\mathbf{CD})_4$ (*m/Z* ($M+3H^+$): calc. 757.7511; obs. 757.3842); inset shows the *m/Z* peaks of the triprotonated $(\mathbf{CD})_4$.

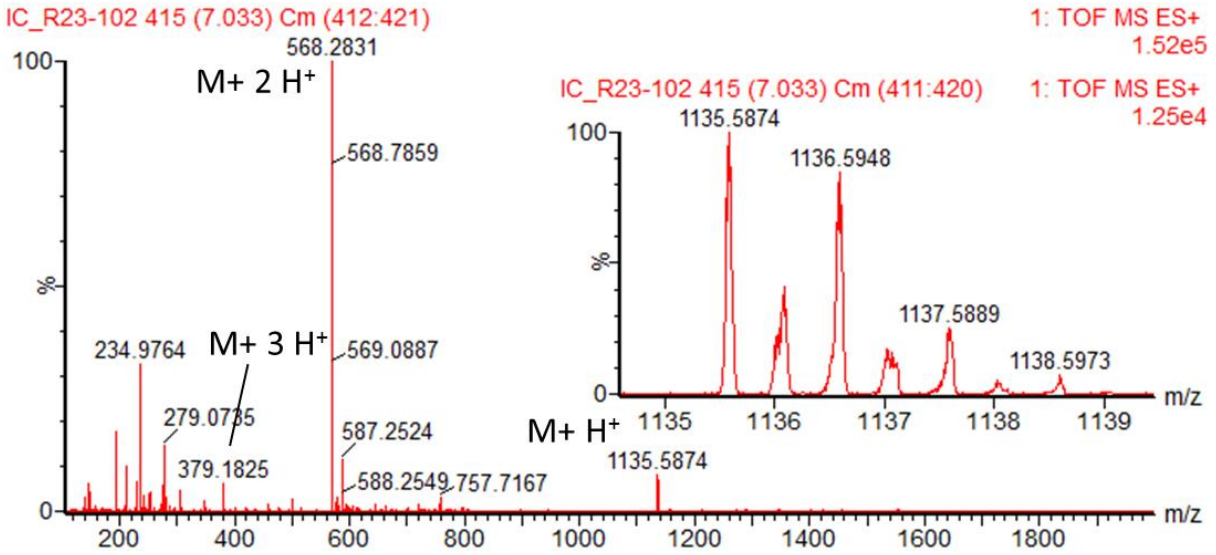

Figure S14. UPLC-MS analysis of library **CD-L1**. Mass spectrum of the peak at 7.03 min, belonging to $(\mathbf{CD})_2$ (*m/Z* ($M+H^+$): calc. 1135.6214; obs. 1135.5874); inset shows the *m/Z* peaks of the monoprotonated $(\mathbf{CD})_2$.

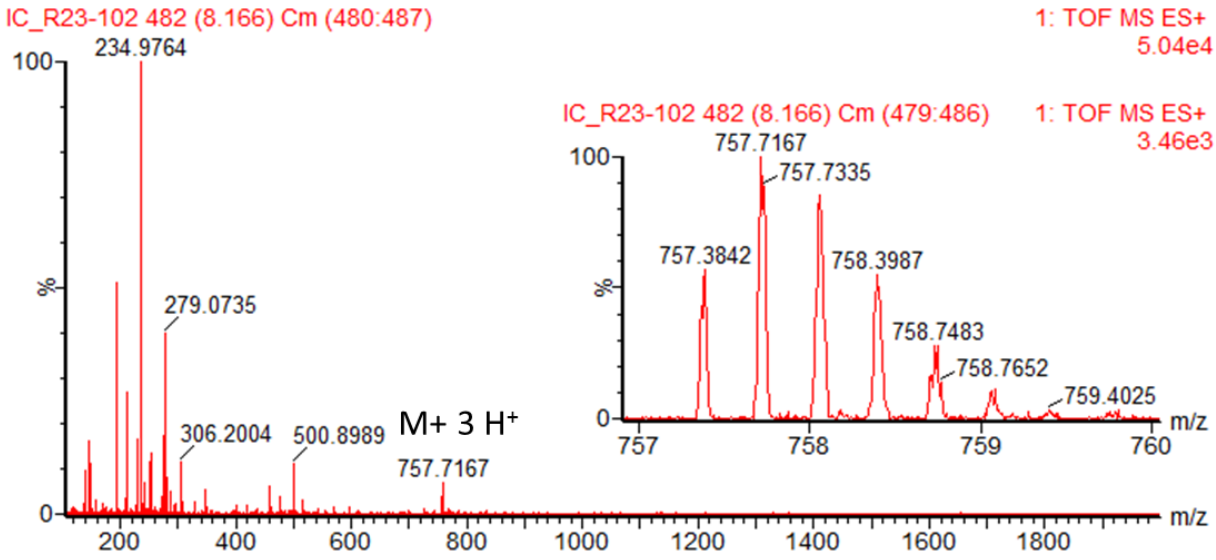

Figure S15. UPLC-MS analysis of library **CD-L1**. Mass spectrum of the peak at 8.17 min, belonging to $(\mathbf{CD})_4$ (*m/Z* ($M+3H^+$): calc. 757.7511; obs. 757.3842); inset shows the *m/Z* peaks of the triprotonated $(\mathbf{CD})_4$.

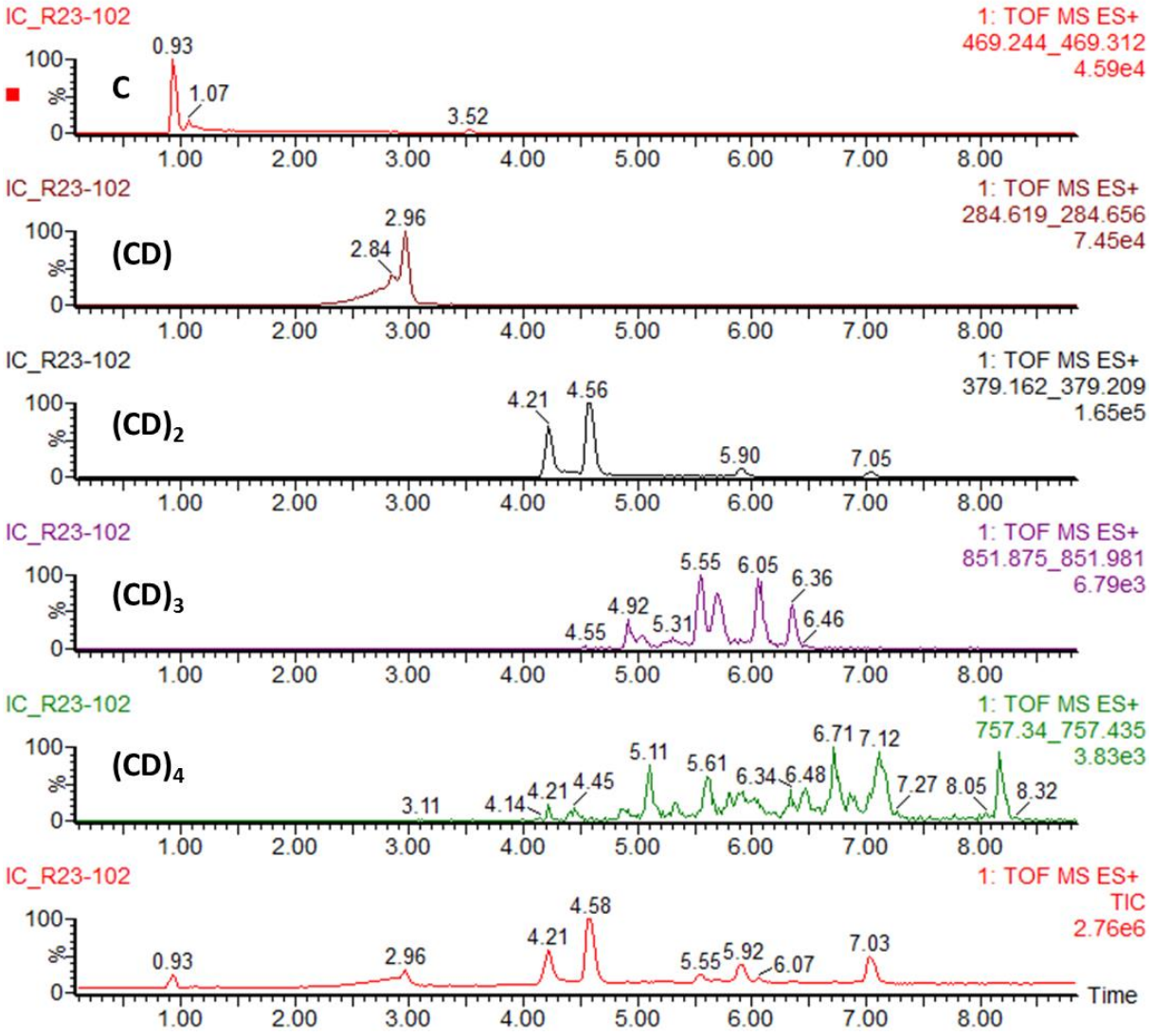

Figure S16. UPLC-MS analysis of library **CD-L1**. Chromatograms monitored at the masses of building block **C** and the (**CD**)$_n$ oligomers, and comparison of the observed signals with the TIC signal (bottom). Analysis reveals two dimers, four tetramers, seven hexamers, and fifteen octamers.

The second library (**CD-L2**) was prepared by dissolving solid mixture of (**CD**)$_n$ oligomers in ammonium acetate buffer (50 mM, pH = 4.0) and irradiating the solution with 365 nm UV light until the photostationary state was reached. In this system only five different tetramers were identified (see Figures S17 and S18, and detailed mass spectra in Figures S19-S23).

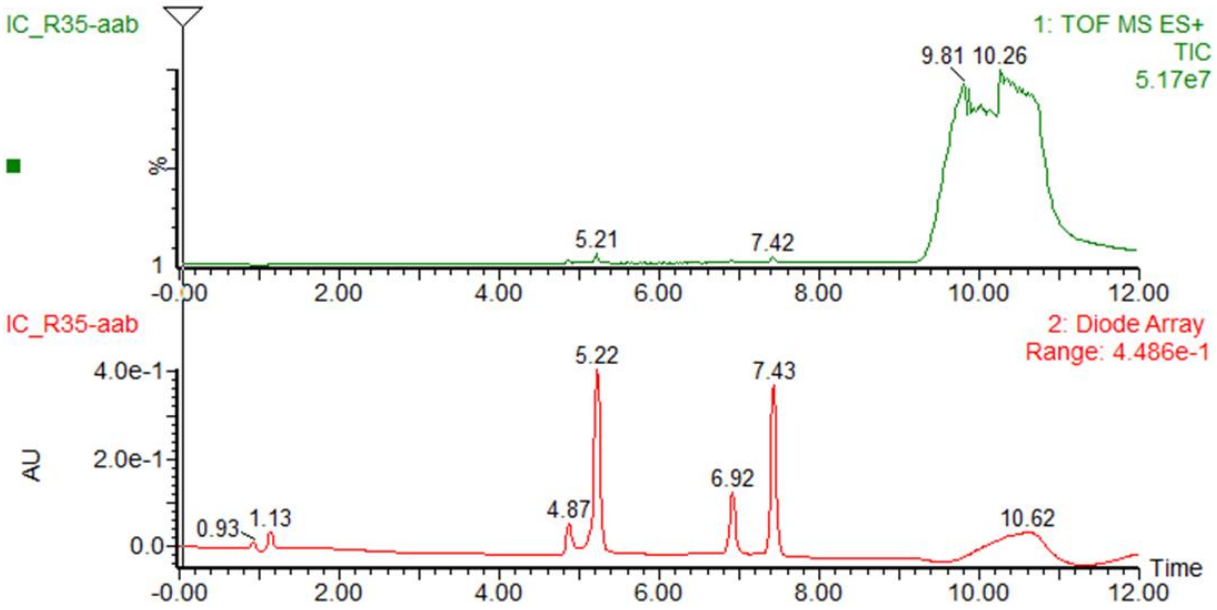

Figure S17. Chromatogram of the (**CD**)$_n$ library **CD-L2**. TIC signal (above) and UV signal (240 nm) (below).

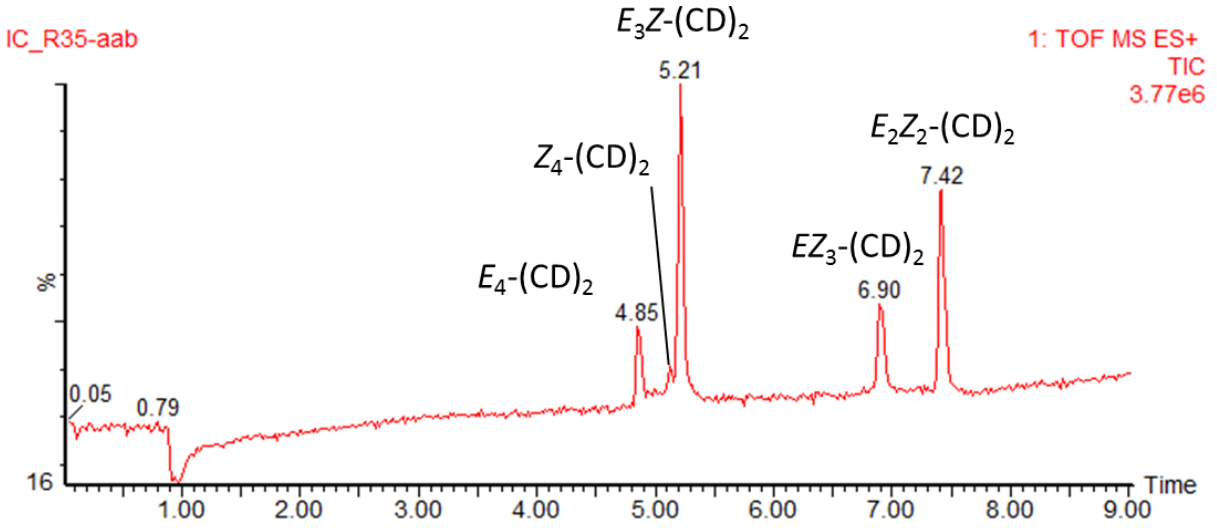

Figure S18. Chromatogram of the (**CD**)$_n$ library **CD-L2**. Expanded region of the TIC signal with assignement of all identified library members.

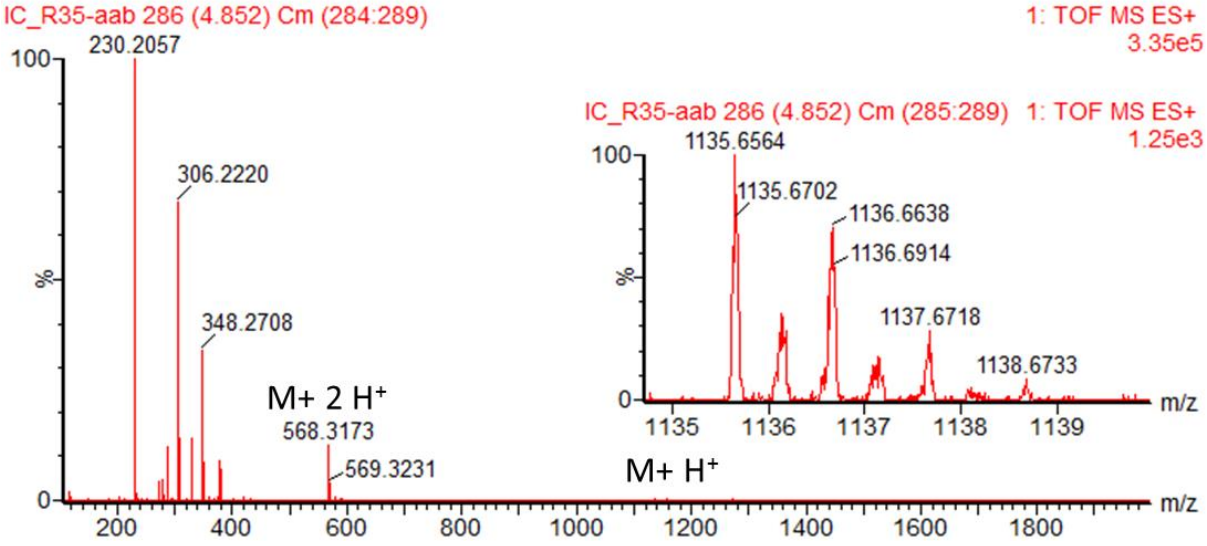

Figure S19. UPLC-MS analysis of library **CD-L2**. Mass spectrum of the peak at 4.85 min, belonging to E_4-(**CD**)$_2$ (*m*/*Z* (M+H$^+$): calc. 1135.6214; obs. 1135.6564); inset shows the *m*/*Z* peaks of the monoprotonated E_4-(**CD**)$_2$.

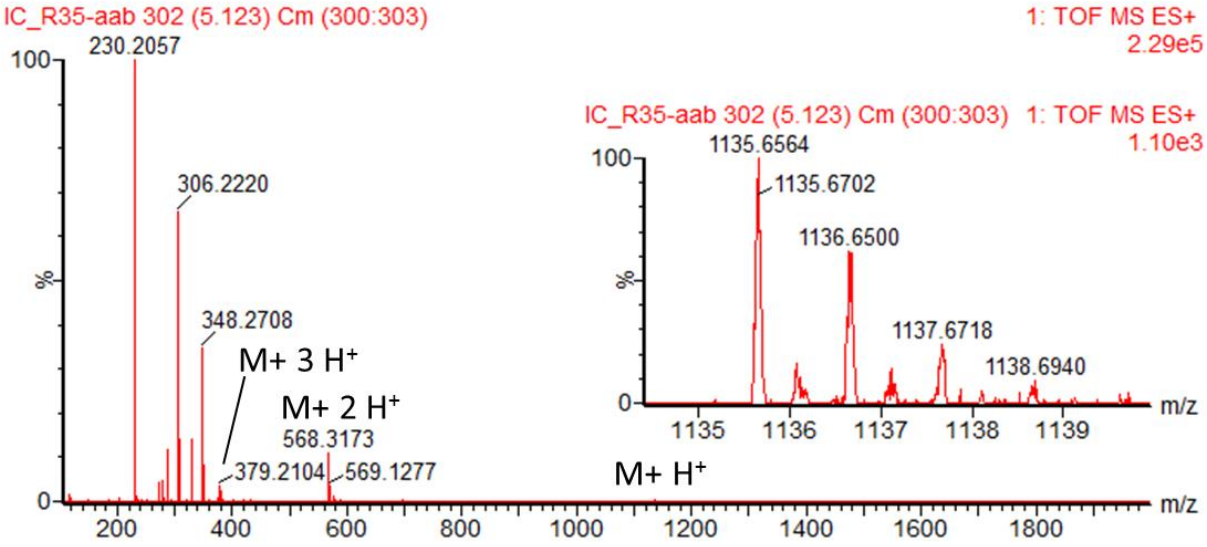

Figure S20. UPLC-MS analysis of library **CD-L2**. Mass spectrum of the peak at 5.12 min, belonging to Z_4-(**CD**)$_2$ (*m*/*Z* (M+H$^+$): calc. 1135.6214; obs. 1135.6564); inset shows the *m*/*Z* peaks of the monoprotonated Z_4-(**CD**)$_2$.

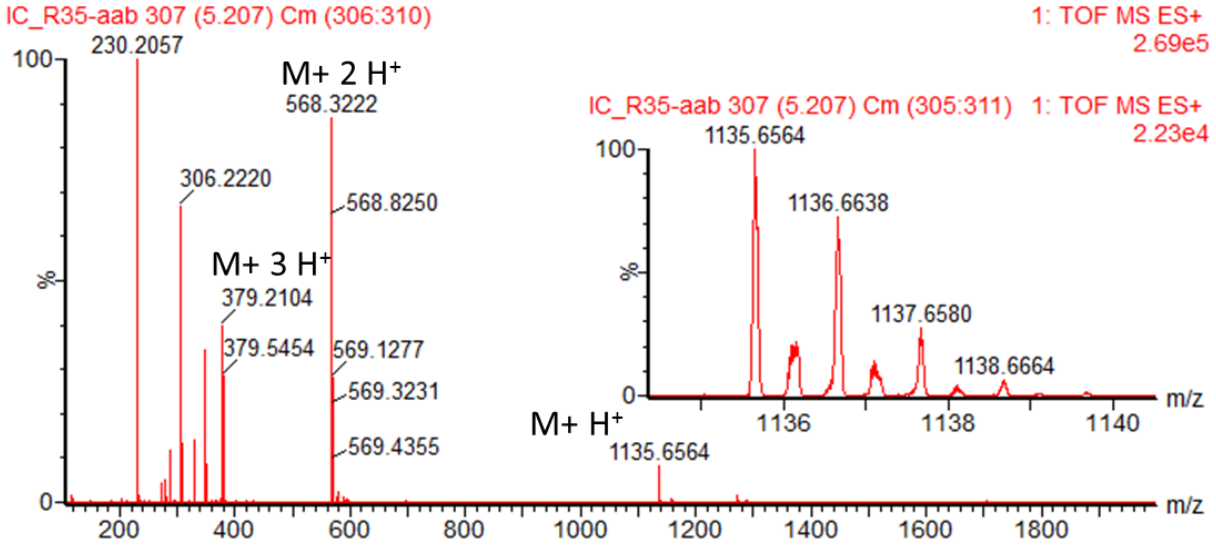

Figure S21. UPLC-MS analysis of library **CD-L2**. Mass spectrum of the peak at 5.21 min, belonging to E_3Z-(**CD**)$_2$ (*m*/*Z* (M+H$^+$): calc. 1135.6214; obs. 1135.6564); inset shows the *m*/*Z* peaks of the monoprotonated E_3Z-(**CD**)$_2$.

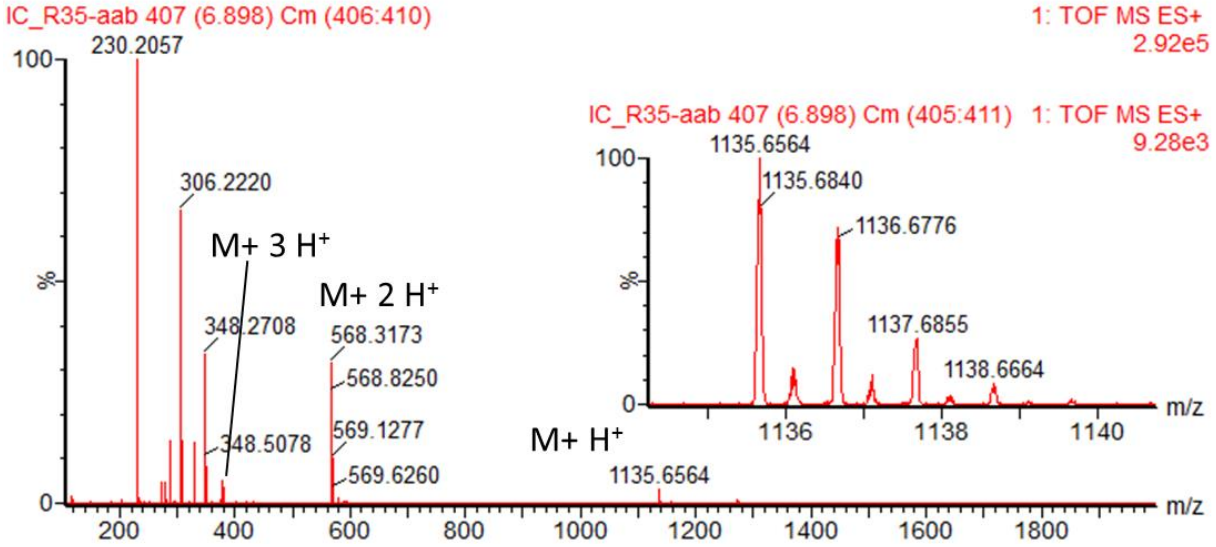

Figure S22. UPLC-MS analysis of library **CD-L2**. Mass spectrum of the peak at 6.90 min, belonging to EZ_3-(**CD**)$_2$ (*m*/*Z* (M+H$^+$): calc. 1135.6214; obs. 1135.6564); inset shows the *m*/*Z* peaks of the monoprotonated EZ_3-(**CD**)$_2$.

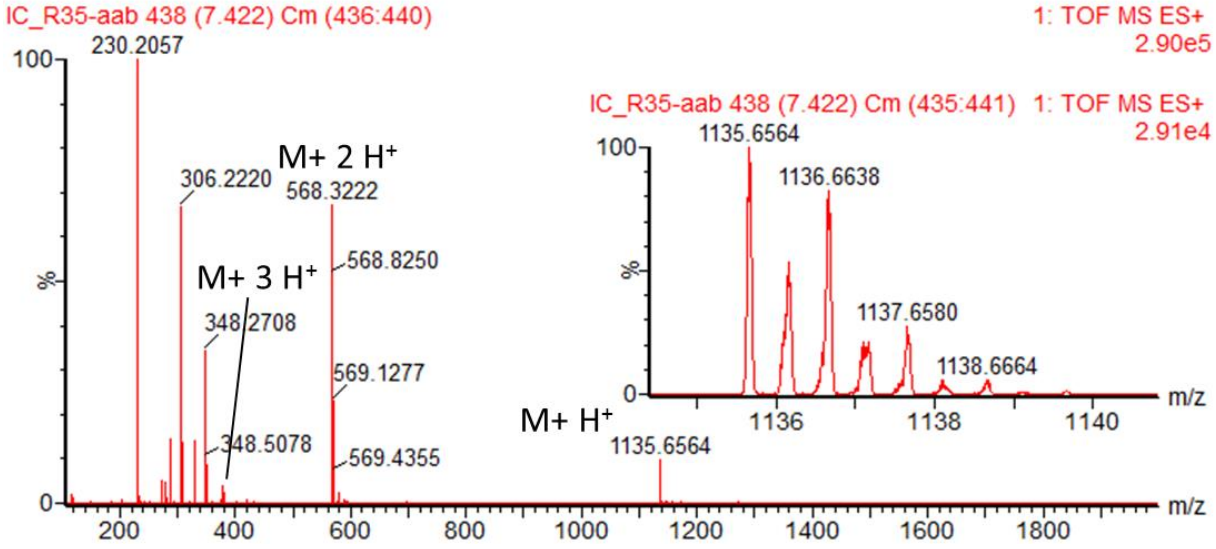

Figure S23. UPLC-MS analysis of library **CD-L2**. Mass spectrum of the peak at 7.42 min, belonging to E_2Z_2-(**CD**)$_2$ (*m*/*Z* (M+H$^+$): calc. 1135.6214; obs. 1135.6564); inset shows the *m*/*Z* peaks of the monoprotonated (E_2Z_2-(**CD**)$_2$.

4. UV irradiation experiments

All UV irradiation experiments were performed using 365 nm UV light from a 2 × 4W table UV lamp (VL-4.LC). During the irradiation the hydrazone solutions were kept in closed 2.0 mL UPLC vials, positioned about 3 cm away from the irradiating tube. Smaller samples were kept in UPLC inserts inside the vials. Samples for UV/Vis spectroscopy were kept in quartz cuvettes. Monitoring compositions of the solutions was performed by UPLC, the samples for analysis being drawn directly from the vials with the irradiated solutions.

Changes in the absorption spectrum of **AB** were analyzed by measuring the the UV/Vis absorption of aqueous solution of **AB** (20 μM), along with irradiating it with 365 nm UV in 2 min (and finally 10 min) steps (Figure S24a).

The photostationary state for concentrated solutions of **AB** was reached after approx. 3h of irradiation of 1.00 mM **AB** dissolved in water, with short breaks when the vial was taken away for UPLC analysis. The *E*:*Z* ratio in the photostationary state was 52:48 (Figure S25a). The UV absorbance was measured at 300 nm. As this was not an isosbestic point, the relative amounts and therefore the concentrations of the two isomers were calculated from the changes in the corresponding peak areas. Namely, as isomerization of **AB** is a 1:1 reaction, the amount for which one isomer decreases during the isomerization equals the amount for which the other isomer increases. Consequently, the ratio of the changes in the peak areas of the two isomers between any two measurements equals the ratio of the corresponding absorbances. The ratio of absorbances used for determining the actual compositions of the monitored samples was calculated by averaging the ratios of changes of peak areas between all pairs of measurements in one of the preliminary experiments.

Changes in the absorption spectrum of the (**CD**)$_n$ oligomers library were analyzed by measuring the UV/VIS absorption of 0.015 mM aqueous solution obtained by diluting equilibrated 0.15 mM library, along with irradiating it with 365 nm UV light in 1 min steps. As the system comprises at least five different species, existence of an isosbestic point was highely unlikely. However, possibly due to the fact that all the species differ only in their *E*/*Z* states, the absorbance did not change significantly at 242 nm and that wavelength was used for UPLC analyses and to quantify the relative amounts of the isomers (Figure S24b).

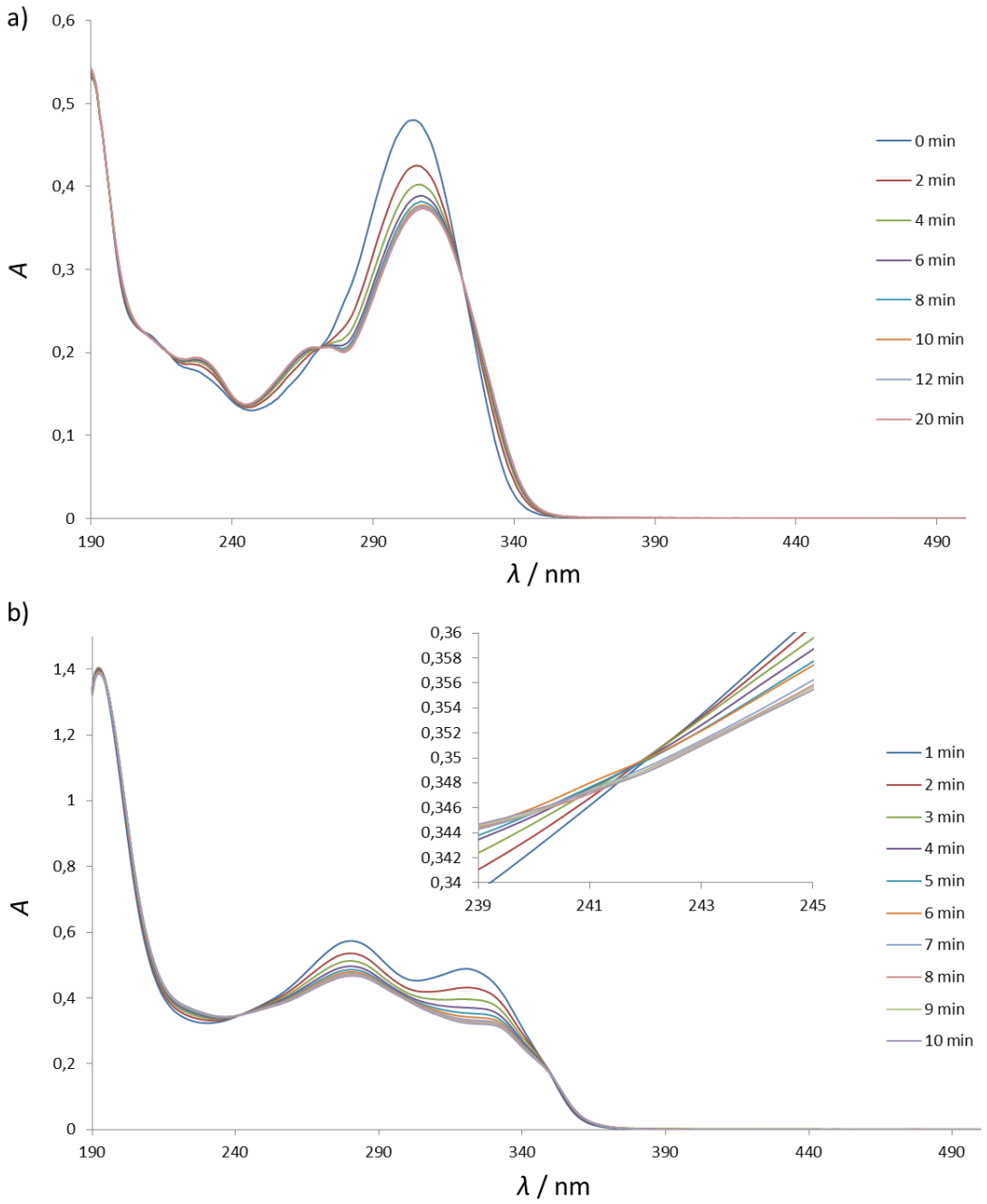

Figure S24. Changes in UV spectra of the hydrazones upon UV irradiation (365 nm): a) **AB**, dissolved in water (20 µM); b) 15 µM aqueous solution of (**CD**)$_n$ oligomers. The inset shows a magnified part of the graph, where the total absorbance stays nearly constant.

The photostationary state of (**CD**)$_n$ library was reached after 55 min of irradiation of a 0.15 mM predominantly (**CD**)$_2$ solution. The irradiation was first performed in 1 min steps, their length gradually extending to 5 min (Figure S25b). The sample was analysed by UPLC after each irradiation step. The UV absorbance was measured at 242 nm and the relative amounts of the isomers were calculated directly from the peak areas, assuming their absorbances at this wavelength were equal.

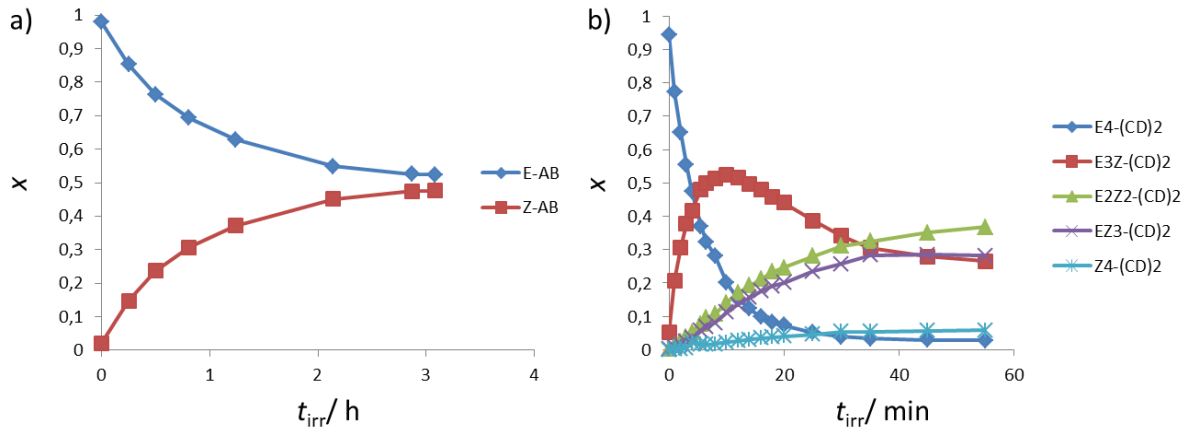

Figure S25. Relative amounts of the hydrazone isomers (expressed as mole fractions, x) during UV irradiation of the solutions of: a) **AB**; b) $(\mathbf{CD})_2$ macrocycles. Experimental conditions as described in text.

5. Nucleophilic catalysis experiments

Nucleophilic catalysis experiments were performed by adding small amounts of nucleophiles to samples of photostationary solutions of linear or macrocyclic hydrazones, and by monitoring the samples by UPLC (see Figure S26 for kinetic profiles of the thermal isomerization). For the **AB** hydrazone this was done by irradiating a 2.0 mM solution of **AB** in 20 mM ammonium acetate buffer until the photostationary state was reached, and then by diluting samples of that solution to 1.0 mM with water, ammonium acetate buffer and aqueous solutions of nucleophiles (except for **11** which was dissolved in EtOH due to its low solubility in water). The macrocyclic system was treated in a similar fashion, but starting with a 0.75 mM library solution and diluting it to 0.25 mM just before the UPLC monitoring. In all experiments UV absorbance was measured at 242 nm. Additionally to the experiments described in the main text, the *Z*→*E* isomerization in the macrocycle system was also monitored in the presence of **13** (Figure S27a), I_2/KI (Figure S27b), and **14** (Figure S27c). Besides that, the effect of pH of the solution on the isomerization rate was investigated, and the results show that the inversion rate increases with the acidity of the solution (Figure S27d). In general, thermal isomerization brings the system back to equilibrium regardless of the catalyst used (Table S2). This was, however, only observed with the most efficient catalysts, as with the others equilibration times are measured in days.

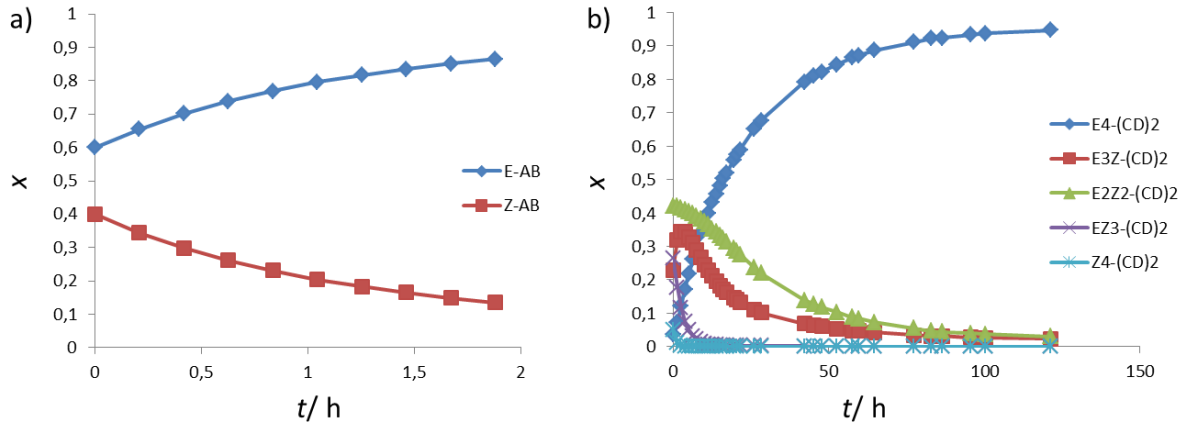

Figure S26. Kinetic profiles of Z → E isomerization of: a) linear hydrazone **AB** (2.0 mM in water); b) macrocyclic hydrazones (0.50 mM in 50 mM ammonium acetate buffer, pH = 4.0). The amounts of the isomers are presented as their mole fractions, x.

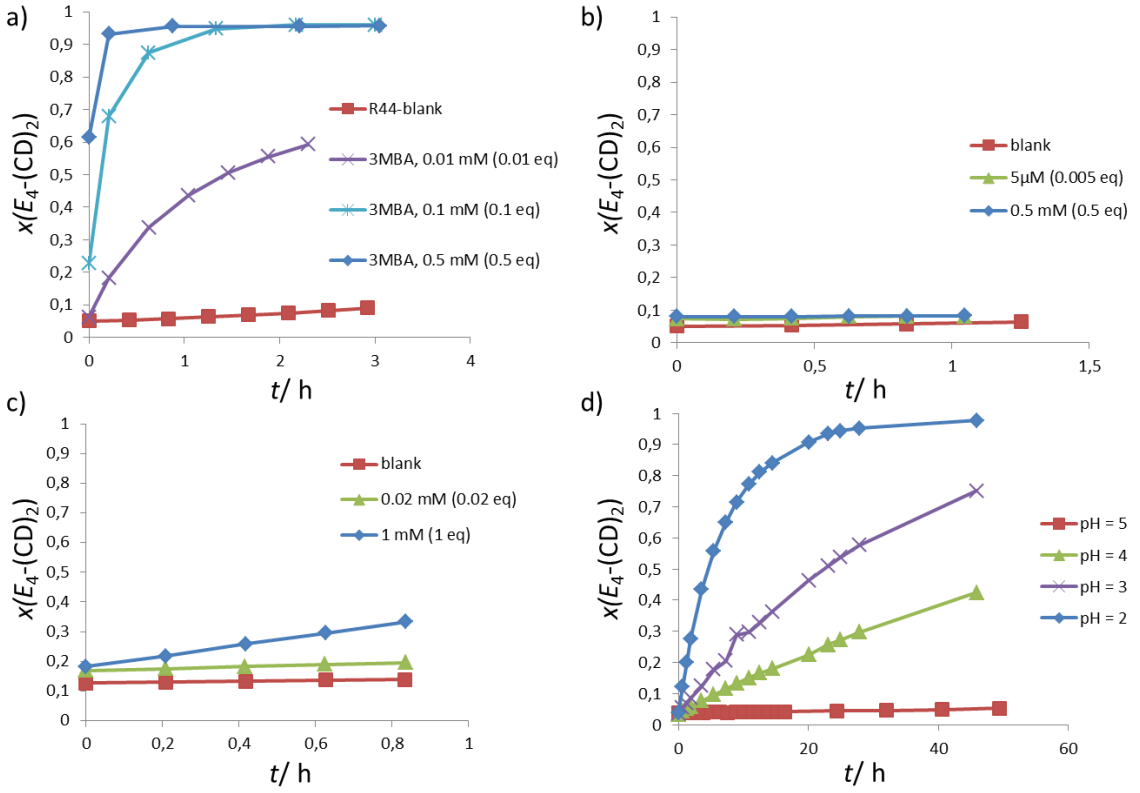

Figure S27. Effects of various compounds and pH on the Z → E isomerization rate: a) **13**; b) I_2/KI; c) TCEP (**14**); d) effect of pH. In all experiments a 0.25 mM solution of (**CD**)$_2$ macrocycles was used. In a-c) they were dissolved in 20 mM ammonium acetate buffer (pH = 4.0), and in d) the pH was controlled by adding 1M HCl to a non-buffered solution. For clarity, only the relative amount of E_4-(**CD**)$_2$ is shown, as its mole fraction, x.

Table S2. Compositions of the equilibrated (**CD**)$_2$ solutions (0.25 mM, 50 mM ammonium acetate buffer, pH = 4) obtained in several different ways.

	$x(E_4$-(**CD**)$_2)$	$x(E_3Z$-(**CD**)$_2)$	$x(E_2Z_2$-(**CD**)$_2)$	$x(EZ_3$-(**CD**)$_2)$	$x(Z_4$-(**CD**)$_2)$
Equilibrated solution, prior to UV	0.944	0.0508	0.00277	0.00175	0.000309
Solution equilibrated by standing for a week	0.947	0.0232	0.0294	0	0
Solution equilibrated by **13** (0.5 mM, 0.5 eq)	0.960	0.0223	0.0182	0	0
Solution equilibrated by **12** (1 mM, 1 eq)	0.966	0.0186	0.0152	0	0
Solution equilibrated by **11** (1 mM, 1eq)	0.956	0.0183	0.0258	0	0

The reaction rates (for the (all)-*E*-isomers) were calculated by fitting the first (linear) parts kinetic traces, and the relative enhancements were determined by dividing the reaction rates in catalyzed reactions with the rates in the blank probes (Table S3). In case of very efficient catalysts (**11-13**) the reaction was too fast to follow by UPLC so the actual enhancements are probably much greater than the estimates suggest.

Table S3. Initial inversion rates and relative enhancements with the tested catalysts.

	AB			**CD**		
Catalyst	Catalyst loading (mM; mol %)	Initial reaction rate (mM / h)	Enhancement	Catalyst loading (mM; mol %)	Initial reaction rate (mM / h)	Enhancement
Blank					$8.60\cdot10^{-5}$	1
1	(20; 20 eq)	0.0911	1	50; 50 eq	$5.00\cdot10^{-3}$	58.1
2				50; 50 eq	$8.56\cdot10^{-3}$	99.4
3				1.0; 1 eq	$7.10\cdot10^{-4}$	8.25
4				1.0; 1 eq	$9.04\cdot10^{-5}$	1.05
5				1.0; 1 eq	$4.17\cdot10^{-4}$	4.85
6	0.5; 0.5 eq	0.1509	1.66	55; 5 eq	0.0602	699
7	1; 1 eq	0.0855	0.939	50; 50 eq	0.0204	236
8 [a]	1; 1 eq	0.0926	1.02	1.0; 1 eq	[a]	[a]
9	1; 1 eq	0.1074	1.18	1.0; 1 eq	0.0148	172
10	1; 1 eq	0.1064	1.17	1.0; 1 eq	0.0104	121
11	1; 1 eq	1.1015	**12.1**	1.0; 1 eq	0.117	**1360**
12	1; 1 eq	0.9106	**10.0**	1.0; 1 eq	0.0844	**981**
13				0.010; 0.01 eq	0.144	**1670**
13				0.10; 0.1 eq	0.542	**6300**
13				0.50; 0.5 eq	0.381	**4430**
14				0.020; 0.02 eq	$8.10\cdot10^{-3}$	94.2
14				1.0; 1 eq	0.0456	530

a) The amount of E_4-(**CD**)$_2$ slightly decreased during the experiment, while the amount of E_2Z_2-(**CD**)$_2$ slightly increased. However, the overall composition remained nearly constant.

6. Modelling of isomerization kinetics

Reflecting the fact that we only observe five (**CD**)$_2$ isomers out of the seven theoretically possible (see Scheme 2c in the main text), a model was developed containing only one E_2Z_2-(**CD**)$_2$ isomer (failure to detect the other two may be either due to their instability, or due to overlap of their peaks in the UPLC analysis). Also, assuming that conformation has small effect on the inversion rates, the rate constants for the formation of the various isomers can be treated as the products of the rate constants of the $E \rightarrow Z$ or $Z \rightarrow E$ isomerization and the number of *E* or *Z* C=N bonds in the molecule (Scheme S2). In this model the composition of the equilibrium mixture depends solely on the k_a/k_b ratio, where k_a and k_b are rate constants for thermal $E \rightarrow Z$ and $Z \rightarrow E$ isomerization, respectively. Analogously, for the photostationary state the composition will be defined by the ratio of rate constants for $E \rightarrow Z$ isomerization during irradiation and the thermal $Z \rightarrow E$ isomerization (k_a^*/k_b). Thus, in this analysis k_a^* contains contributions from both the photochemical and thermal $E \rightarrow Z$ pathways.

$$E_4\text{-(CD)}_2 \underset{k_b}{\overset{4 \cdot k_a}{\rightleftharpoons}} E_3Z\text{-(CD)}_2 \underset{2 \cdot k_b}{\overset{3 \cdot k_a}{\rightleftharpoons}} E_2Z_2\text{-(CD)}_2 \underset{3 \cdot k_b}{\overset{2 \cdot k_a}{\rightleftharpoons}} EZ_3\text{-(CD)}_2 \underset{4 \cdot k_b}{\overset{k_a}{\rightleftharpoons}} Z_4\text{-(CD)}_2$$

Scheme S2. Simplified model for the observed kinetics of the isomerization of the tetramers.

The composition of the hydrazone libraries can be deduced from the rate constants by taking into account that in equilibrium the ratios of amounts of the consecutive products will be equal to the ratios of the corresponding rate constants:

$[E_4\text{-(CD)}_2]/[E_3Z\text{-(CD)}_2] = k_b/(4 \cdot k_a)$

$[E_3Z\text{-(CD)}_2]/[E_2Z_2\text{-(CD)}_2] = (2 \cdot k_b)/(3 \cdot k_a)$

$[E_2Z_2\text{-(CD)}_2]/[EZ_3\text{-(CD)}_2] = (3 \cdot k_b)/(2 \cdot k_a)$

$[EZ_3\text{-(CD)}_2]/[Z_4\text{-(CD)}_2] = (4 \cdot k_b)/k_a$

From these equations, equations for the amounts of the (**CD**)$_2$ macrocycles in the equilibrated (or photostationary) library can be derived, taking into account that the total amount of the (**CD**)$_2$ macrocycles is constant:

$[E_4\text{-(CD)}_2] + [E_3Z\text{-(CD)}_2] + [E_2Z_2\text{-(CD)}_2] + [EZ_3\text{-(CD)}_2] + [Z_4\text{-(CD)}_2] = c_{total}((CD)_2)$

$[E_4\text{-(CD)}_2] = c_{total}((CD)_2)/(1 + (k_a/k_b)^4)$

$[E_3Z\text{-(CD)}_2] = [c_{total}((CD)_2) \cdot 4 \cdot k_a]/[k_b \cdot (1 + (k_a/k_b)^4)]$

$[E_2Z_2\text{-(CD)}_2] = [c_{total}((CD)_2) \cdot 6 \cdot k_a^2]/[k_b^2 \cdot (1 + (k_a/k_b)^4)]$

$[EZ_3\text{-(CD)}_2] = [c_{total}((CD)_2) \cdot 4 \cdot k_a^3]/[k_b^3 \cdot (1 + (k_a/k_b)^4)]$

$[Z_4\text{-(CD)}_2] = [c_{total}((CD)_2) \cdot k_a^4]/[k_b^4 \cdot (1 + (k_a/k_b)^4)]$

In an initial analysis, the relative rates of singular C=N bond inversion in the **AB** hydrazone was used. From the observed *E*/*Z* ratio of equilibrated **AB** of 90:10, and the *E*/*Z* ratio of 52:48 in the photostationary state the following ratios are obtained:

$k_a/k_b = 0.111$

$k_a^*/k_b = 0.923$

Using these ratios to model the macrocyclic **CD** system yields compositions of the equilibrated and photostationary libraries that are already starting to approximate the experimentally obtained data (Table S4). Discrepancies, especially for the thermally equilibrated library, show that in the macrocyclic hydrazone the *Z* C=N bonds are less stable than in the linear hydrazone, relative to the *E* C=N bonds. This is most likely a consequence of strain in the macrocycle building up due to $E \rightarrow Z$ isomerization.

In a subsequent analysis we used curve fitting (employing the Berkeley Madonna (BM) software package) to fit the k_a/k_b and k_a*/k_b ratios. Allowing these ratios to deviate from the ones of the **AB** system gave an improved agreement to the experimental data (see Table S4), with the forth and back reactions rate constants ratios changing to:

$k_a/k_b = 0.0248$

$k_a^*/k_b = 1.12$

As experimentally obtained data for the decay of Z_4-(**CD**)$_2$ fit well to a first order reaction (the total concentration dropping beyond detectabity within hours), the rate constant for the first $Z \rightarrow E$ step could be estimated:

$4 \cdot k_b = 0.0202$ / min

$k_b = 5.05 \cdot 10^{-3}$ / min

From this value rate constants for the thermal and photoinduced $E \rightarrow Z$ reaction can then also be calculated:

$k_a = 1.25 \cdot 10^{-4}$ / min

$k_a^* = 5.66 \cdot 10^{-3}$ / min

Altogether, the modelling, based on only two adjustable parameters, shows that the data conform to the model which comprises five consecutive isomers, with one of the four C=N bonds being isomerized in each step.

Table S4. Comparison of experimentally determined and predicted compositions of equilibrated and photostationary macrocyclic libraries.

	$x(E_4\text{-}(\mathbf{CD})_2)$	$x(E_3Z\text{-}(\mathbf{CD})_2)$	$x(E_2Z_2\text{-}(\mathbf{CD})_2)$	$x(EZ_3\text{-}(\mathbf{CD})_2)$	$x(Z_4\text{-}(\mathbf{CD})_2)$	Total *E*/*Z* ratio
Equilibrated solution, prior to UV irradiation	**0.944**	**0.0508**	**0.00277**	**0.00175**	**0.000309**	**98:2**
Prediction based on equilibrated **AB**	0.656	0.292	0.0486	0.0036	0.0001	90:10
Prediction based on curve fit in BM	0.907	0.0900	0.00335	$5.54\cdot10^{-5}$	$3.44\cdot10^{-7}$	98:2
Photostationary solution	**0.0350**	**0.229**	**0.422**	**0.264**	**0.0508**	**48:52**
Prediction based on photostationary **AB**	0.0731	0.270	0.374	0.230	0.0531	52:48
Prediction based on curve fit in BM	0.0492	0.221	0.372	0.279	0.0783	47:53

7. Control of *E*/*Z* state by UV irradiation and the oxidation state of the catalyst

7.1. Restorability of the catalyst

In the first experiment, with stopping and restarting isomerization (Figure S28, Figure 3a in the main text), first 0.75 mM photostationary solution of (**CD**)$_2$ isomers in 50 mM ammonium acetate buffer was diluted to 0.25 mM and a 60 µL sample was monitored by UPLC for about an hour (five 1.0 µL injections with UPLC runs lasting 12 min each). Then 1.0 µL of a 0.15 mM aqueous solution of **13** was added to the sample (final concentration of **13** is 2.5 µM) and the monitoring was continued for another hour, after which 1.0 µL of a 0.062 mM I_2/KI solution was added to the sample (final concentration of I_2 is 1.25 µM), with monitoring continued for one more hour. In the last step 1.0 µL of a 0.056 mM of **14** was added (final concentration of **14** is 1.25 µM) and the sample was then monitored for two more hours. The slight excesses of iodine and **14** due to dilution were intentional, to ensure the reduction and oxidation would be complete.

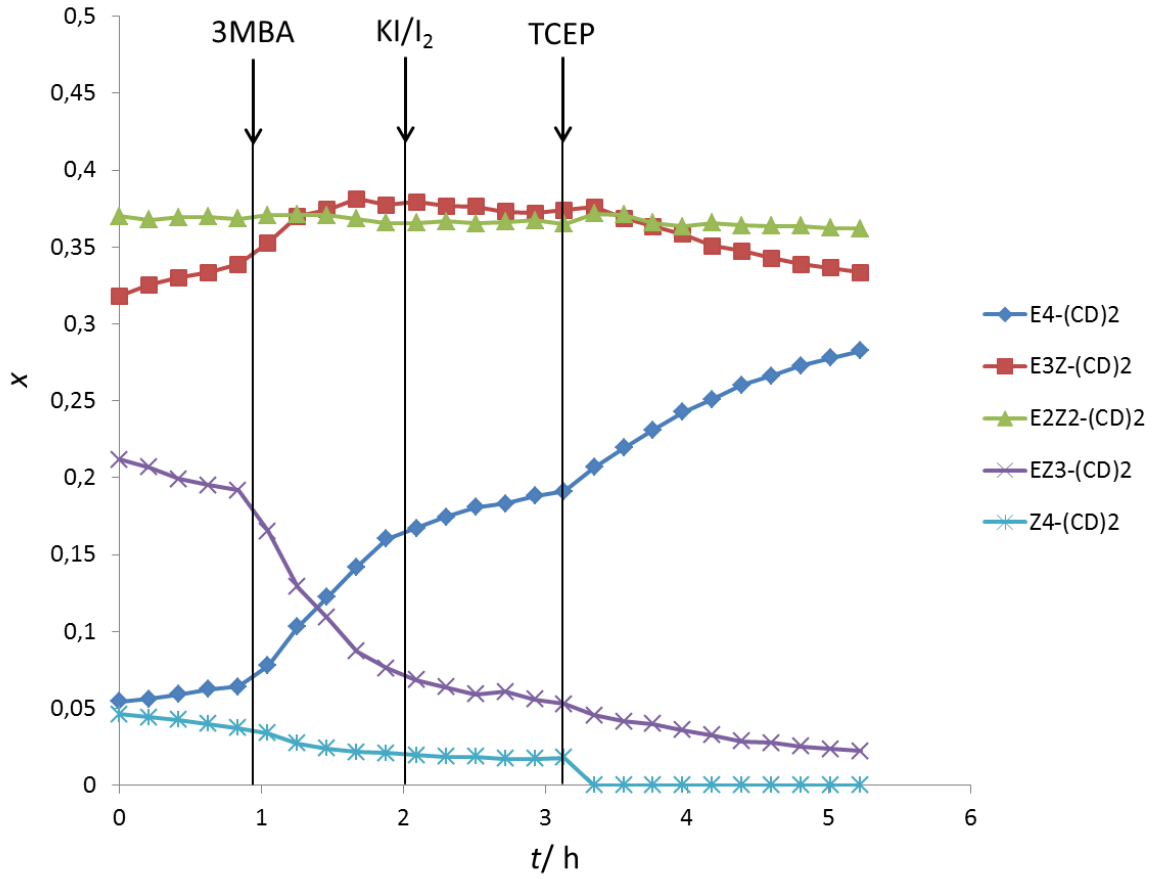

Figure S28. Relative amounts of the five (**CD**)$_2$ isomers during the experiment in which isomerization is stopped and restarted by deactivation and reactivation of the catalyst. Experimental details are provided in the text. The amounts of the isomers are presented as their mole fractions, x.

7.2. Effect of the oxidation state of the catalyst

The effect of the oxidation state was tested by adding the same amount of **13** to the photostationary macrocyclic hydrazone library, but in various states of oxidation of the thiol (Figure S29). This was achieved by mixing the thiol with KI/I_2 solution prior to adding it to the photostationary solution. For this, first 0.15 mM hydrazone library in ammonium acetate buffer was prepared and irradiated until it reached the photostationary state. To the resulting mixture **13** was added, either alone, or about a minute earlier pre-mixed with KI/I_2 solution. The final total concentration of **13** in the hydrazone libraries was 6 µM (1 % catalyst loading, relative to the hydrazone functional groups). Taking into account slow evaporation of iodine from KI/I_2 solution, **13** was oxidized for 40 %, 80 %, and 100 % (with 160 % of I_2).

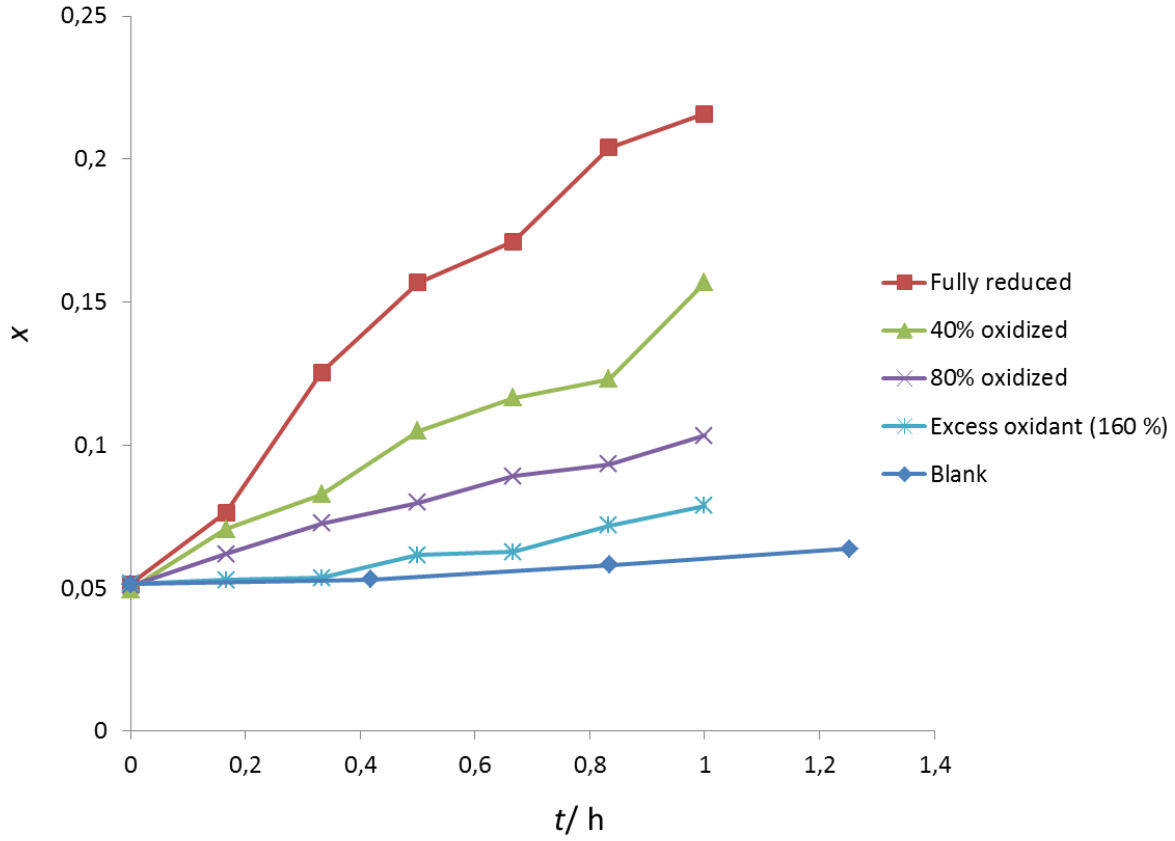

Figure S29. Effect of the oxidation state of the thiol **13** upon the isomerization rates in the hydrazone library. For clarity only the mole fraction (x) of E_4-(**CD**)$_2$ is shown. Experimental details are provided in the main text.

7.3. Compatibility of nucleophilic catalyst with photoisomerization

The third experiment, in which the system was also reverted again to the photostationary state (Fig S30), was performed nearly in the same way, starting with 90 µL sample, which was monitored for an hour. Next, 1.0 µL of a 0.425 mM aqueous solution of **13** (final concentration of **13** is 5.0 µM) was added and the sample was monitored for another hour. Then 1.0 µL of a 0.212 mM aqueous solution of I_2/KI (final concentration of I_2/KI is 2.65 µM) was added, with another hour of monitoring

afterwards. Then the sample was irradiated in two 10 min sessions, using 365 nm UV light, and monitored again for an hour before 1.0 µL of 0.189 mM aqueous solution of **14** (final concentration of **14** is 2.8 µM) was added, with two more hours of subsequent monitoring.

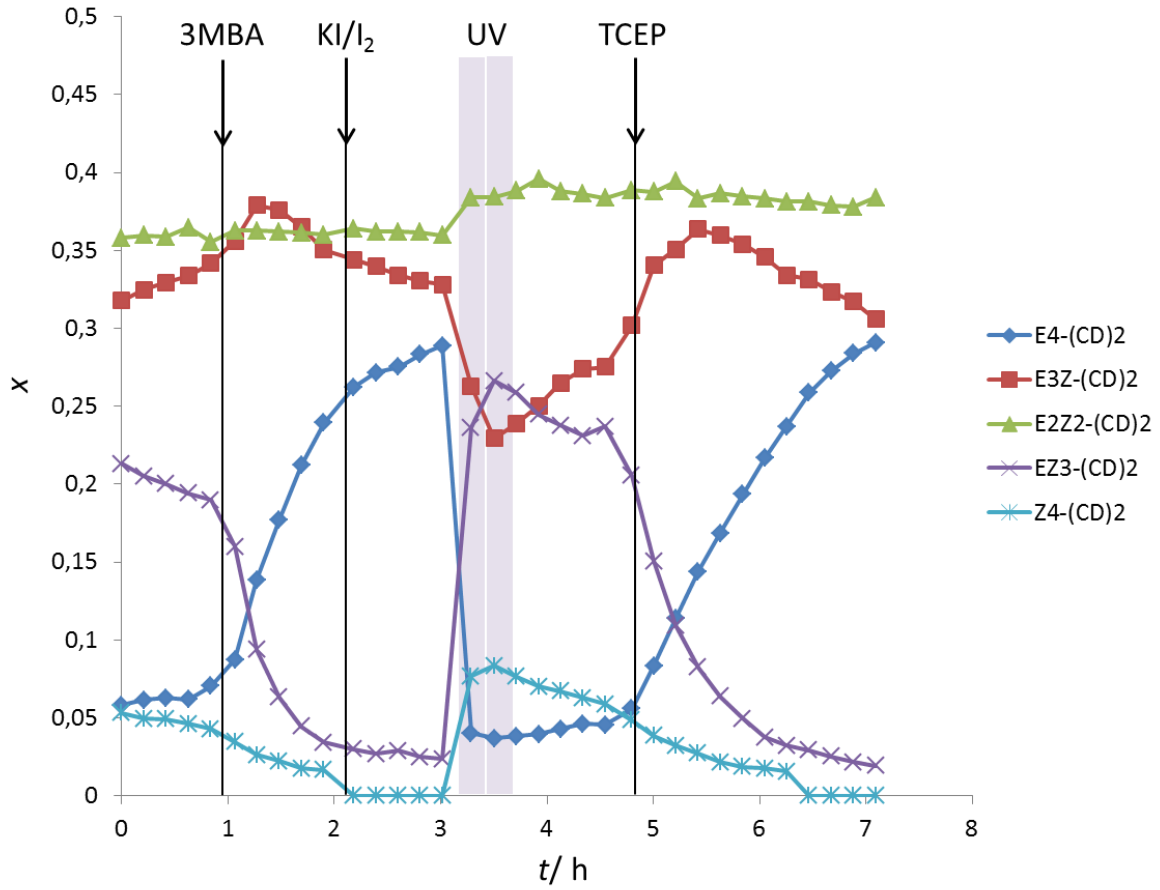

Figure S30. Relative amounts of the five (**CD**)$_2$ isomers during the experiment experiment in which isomerization is stopped and restarted, together with reverting system to photostationary state. Experimental details are provided in the text. The amounts of the isomers are presented as their mole fractions, x.

7.4. Switching cycles on AB hydrazone

Switching cycles (Figure S31) were performed on a 1.0 mM solution of **AB** in aqueous ammonium acetate buffer (20 mM, pH = 4). First, a photostationary solution was prepared by irradiating the sample for three or more hours (up to overnight) with 365 nm UV light. To this solution 0.040 mM (4.0 %) of **13** was added and then the sample was monitored by UPLC until close to equilibrium. Six switching cycles were then performing by irradiating the near-equilibrated sample, and then monitoring it by UPLC. Twice 1 eq. of TCEP was added, to ensure that the thiol stays in its reduced state. In the final step 600 % iodine was added (as KI/I_2 solution).

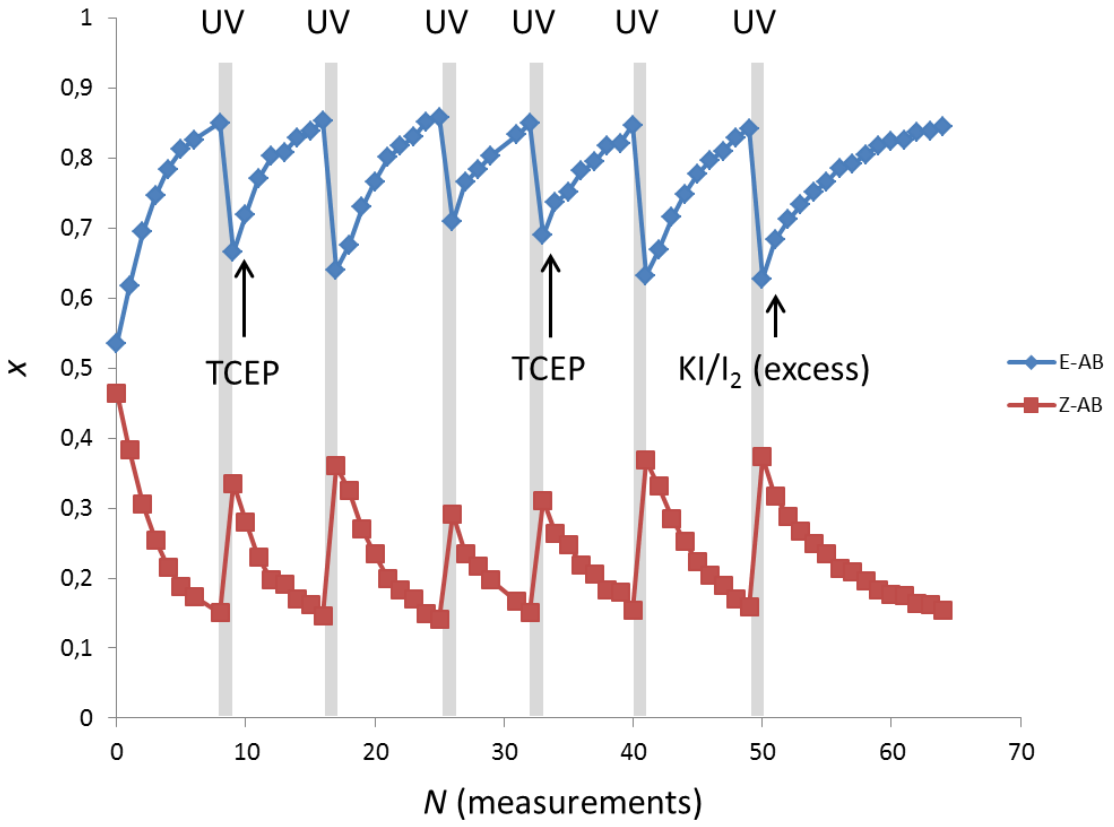

Figure S31. Switching cycles on **AB** (1.0 mM, 20 mM ammonium acetate buffer, pH = 4). Time interval between each two measurements is 10 min, except during the irradiation period, when the sample was left overnight. X represents the mole fraction of *E*- or *Z*-**AB**.

8. Literature

[S1] van Dijken, D. J.; Kovaríček, P.; Ihrig, S. P.; Hecht, S. *J. Am. Chem. Soc.* **2015**, *137*, 14982–14991.